# Discrete Breathers in Hydrogenated Metals:

# Atomistic Simulations and Applications to the Rate Theory

Vladimir Dubinko[1,4], Denis Laptev[2,4], Dmitry Terentyev[3], Klee Irwin[4]

[1]NSC Kharkov Institute of Physics and Technology, Ukraine

[2]B. Verkin Institute for Low Temperature Physics and Engineering, Ukraine

[3]SCK•CEN, Nuclear Materials Science Institute, Mol 2400, Belgium

[4]Quantum Gravity Research, USA

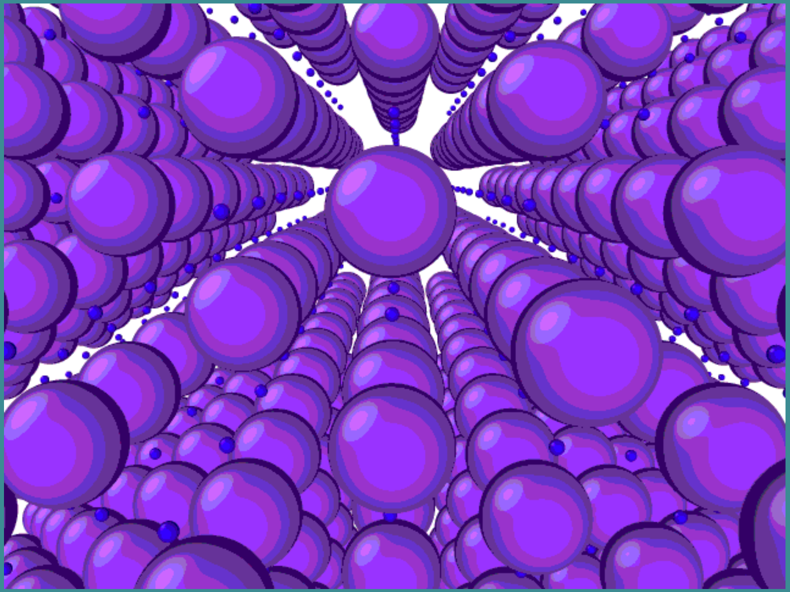

Tartu 2018

# Outline

- DBs/ILMs in metals
- DB role in catalysis at high T (violation of Arrhenius low)
- DB role in catalysis at low T (quantum tunneling)
- MD simulations in Ni, Pd, Ni-H, Pd-H crystals and Pd nanoclusters (3d DB)

# **DBs in metals** Hizhnyakov et al (2011)

PREDICTION OF HIGH-FREQUENCY INTRINSIC . . .

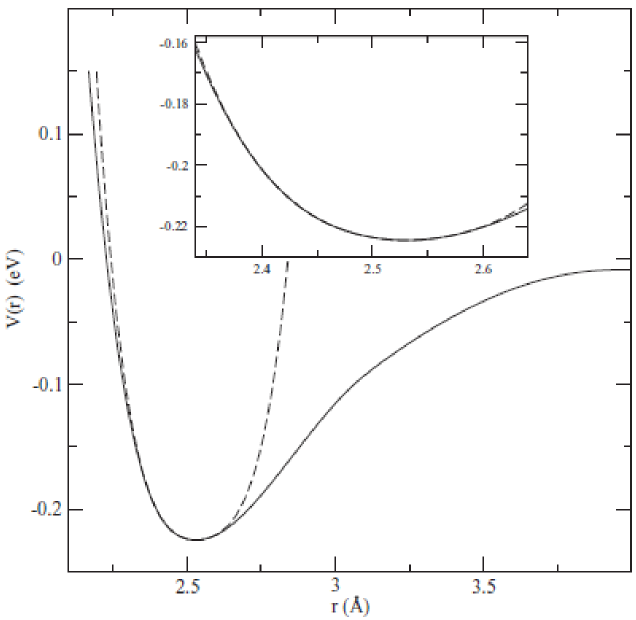


FIG. 1. The pair potential $V(r)$ of Ni (solid line) and its approximation by the fourth-order polynomial (dashed line). The inset shows an expanded view.

The distance between the nearest atoms in Ni at room temperature is $r_0 = 2.49$ Å and longitudinal sound velocity is $v_l = 5266$ m/s. These values give $\tilde{K}_2 = 2.75$ eV/Å$^2$ (as expected, $\tilde{K}_2 > K_2$) and $\tilde{\kappa} \approx 1.2$. The distance $r_0$ increases

HAAS, HIZHNYAKOV, SHELKAN, KLOPOV, AND SIEVERS

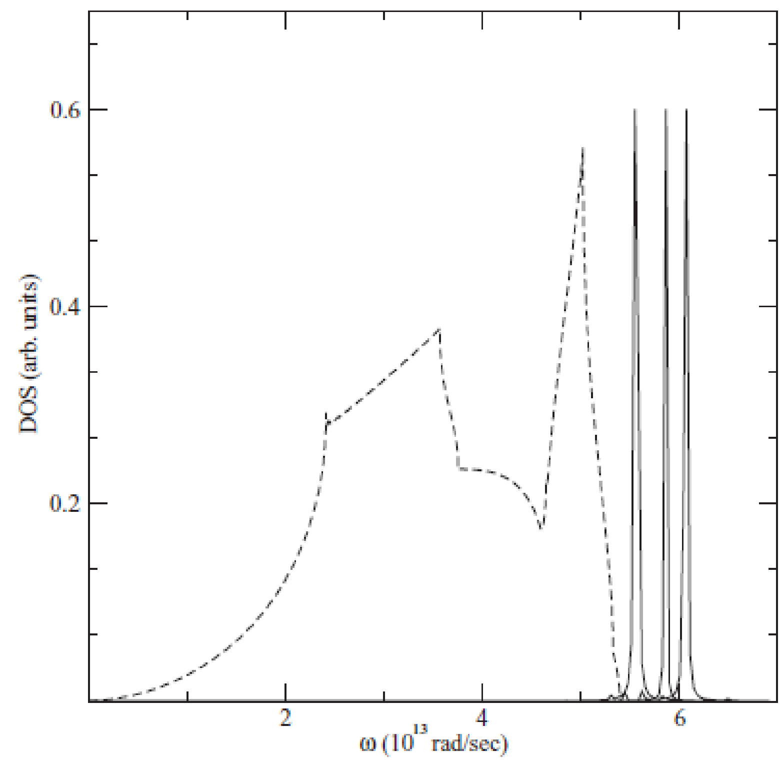


FIG. 2. Phonon density of states and three ILM spectral signatures for Ni. Phonon spectrum (dashed line) and spectrographs (solid line) of the different ILM's: The frequencies are 5.58, 5.86, and 6.07 ($10^{13}$ rad/s) and the amplitudes of vibrations of the central bond are 0.18, 0.31, and 0.42 Å.

**Standing DB in bcc Fe: $d_0$=0.3 Å**

D.Terentyev, V. Dubinko, A. Dubinko (2013)

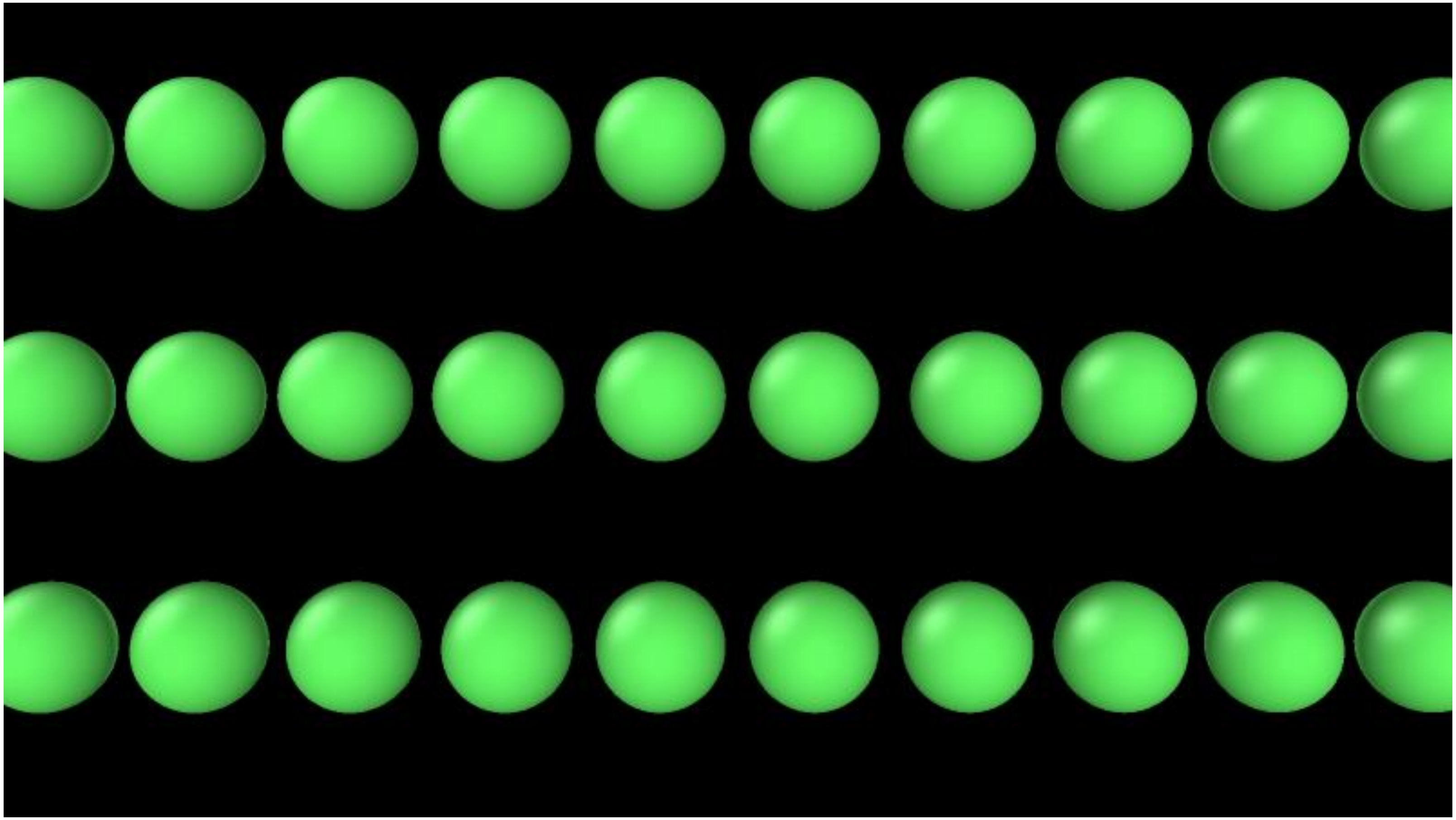

# DB along [111] direction in bcc Fe at T=0K

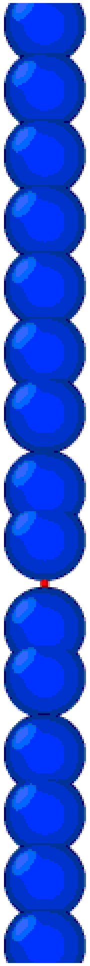

Modelling Simul. Mater. Sci. Eng. **23** (2015) 085007 D A Terentyev *et al*

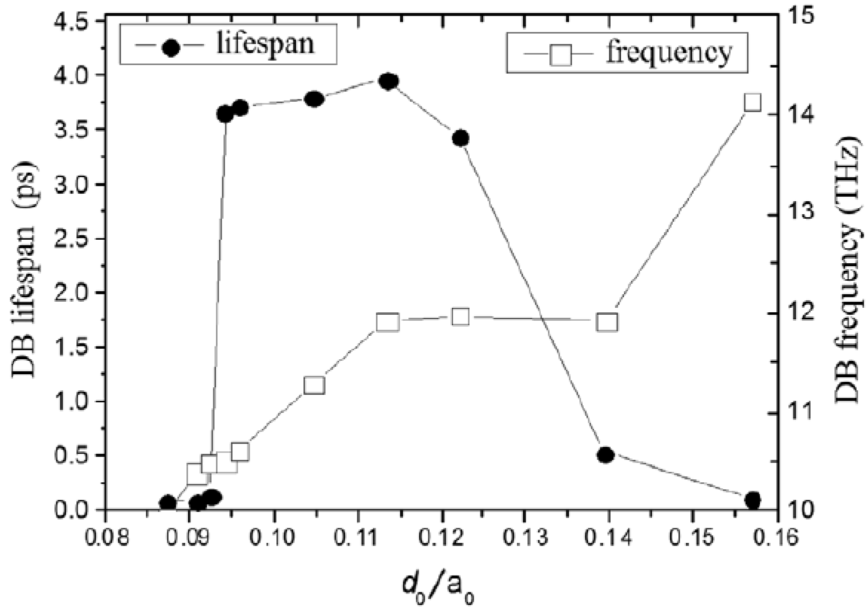


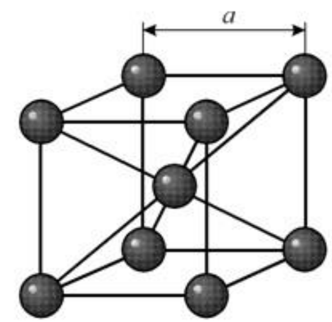


**Figure 1.** Lifespan and frequency of standing DB as the function of the relative initial displacement $d_0/a_0$ for the IAP derived in [28].

**Initial conditions**:

$$x_{n-2} = +0.2 \quad x_{n-1} = -0.2 \quad x_n = +0.4 \quad x_{n+1} = -0.4 \quad x_{n+2} = +0.2 \quad x_{n+3} = -0.2$$

**Boundary conditions**: periodic

**It is seen from the visualization, that the DB has been generated from the initial anti-phase displacements of 6 atoms.**

**Moving DB in bcc Fe: $d_0$=0.4 Å, E= 0.3 eV**

D.Terentyev, V. Dubinko, A. Dubinko (2013)

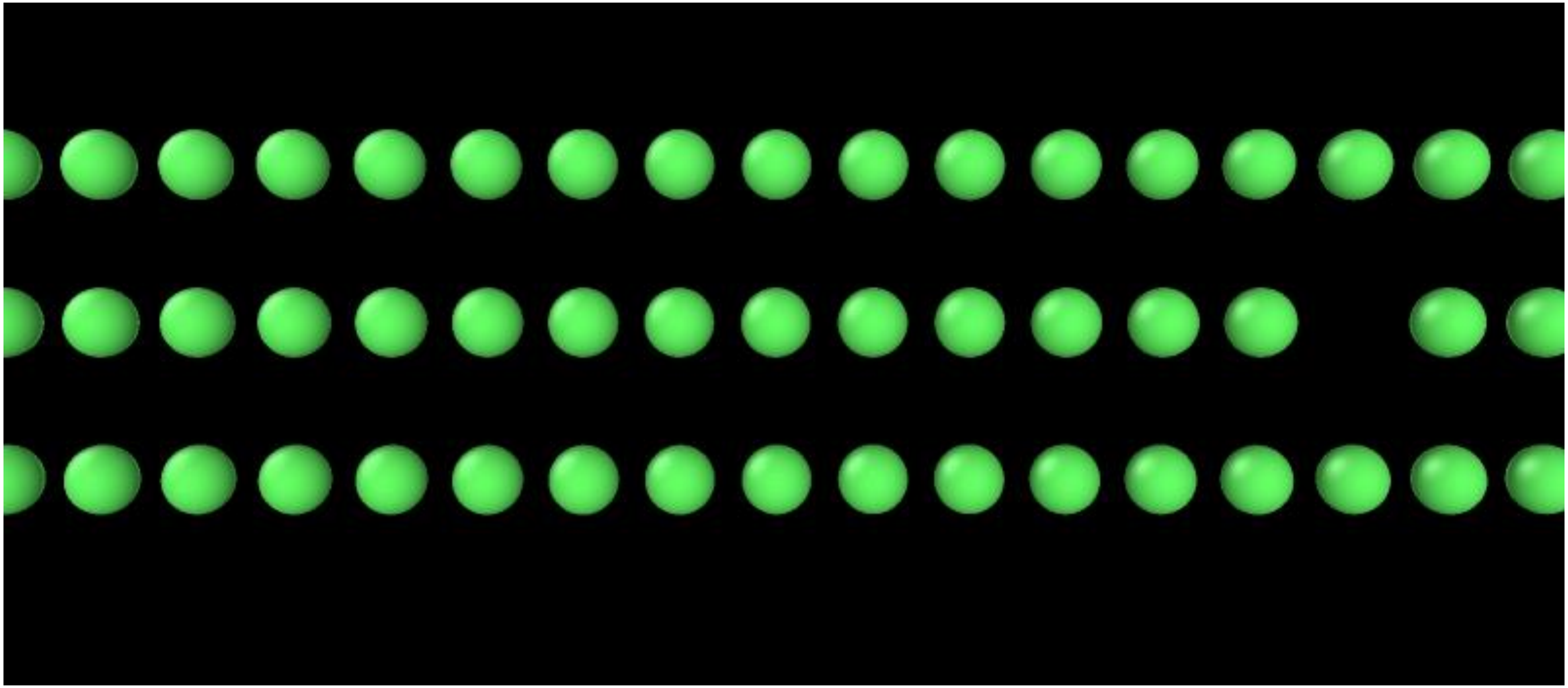

# DB in bulk Pd 3D lattice (2017)

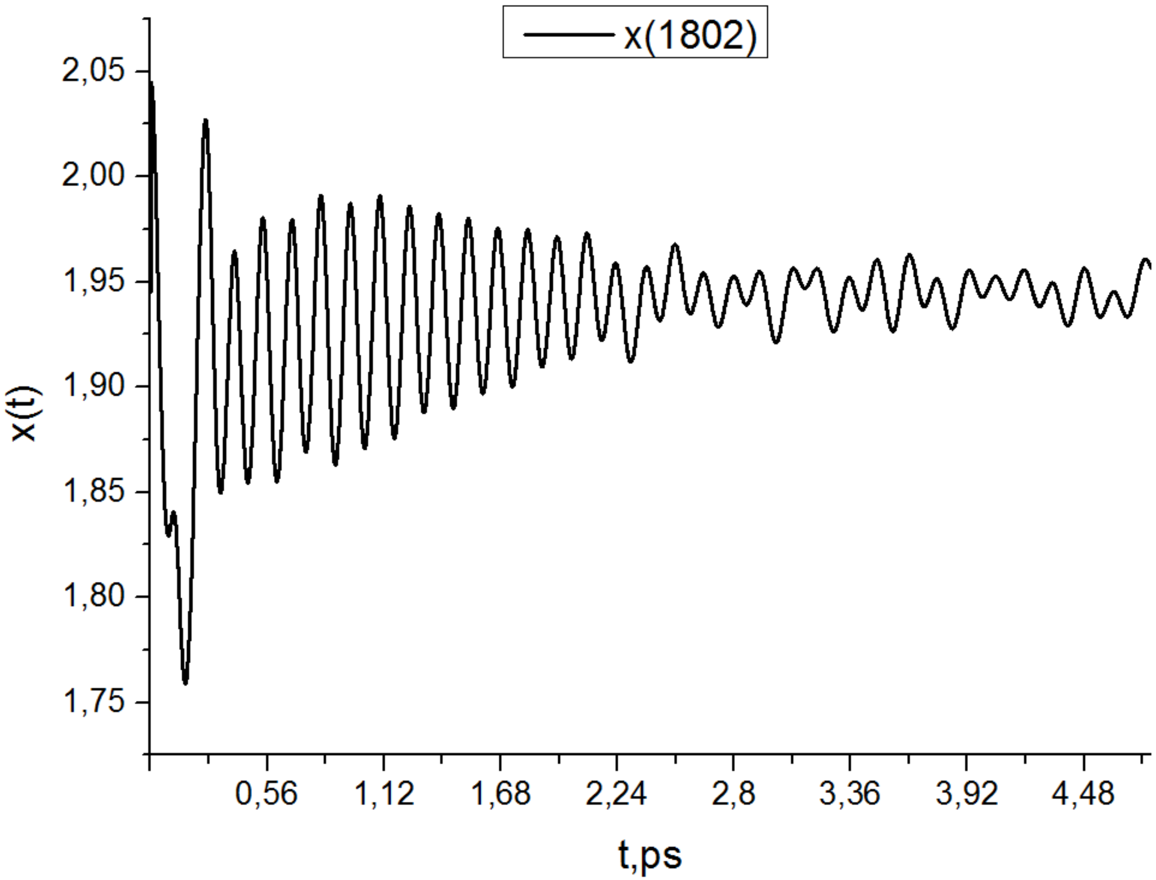


LAV Time Period=
0.1292 ps
LAV frequency =
7.7399 THz

**The DB frequency lies above the phonon vibration spectrum**

# Effective ‘temperature’ of DB (#1100) and lattice (#1095) atom in fcc Pd lattice

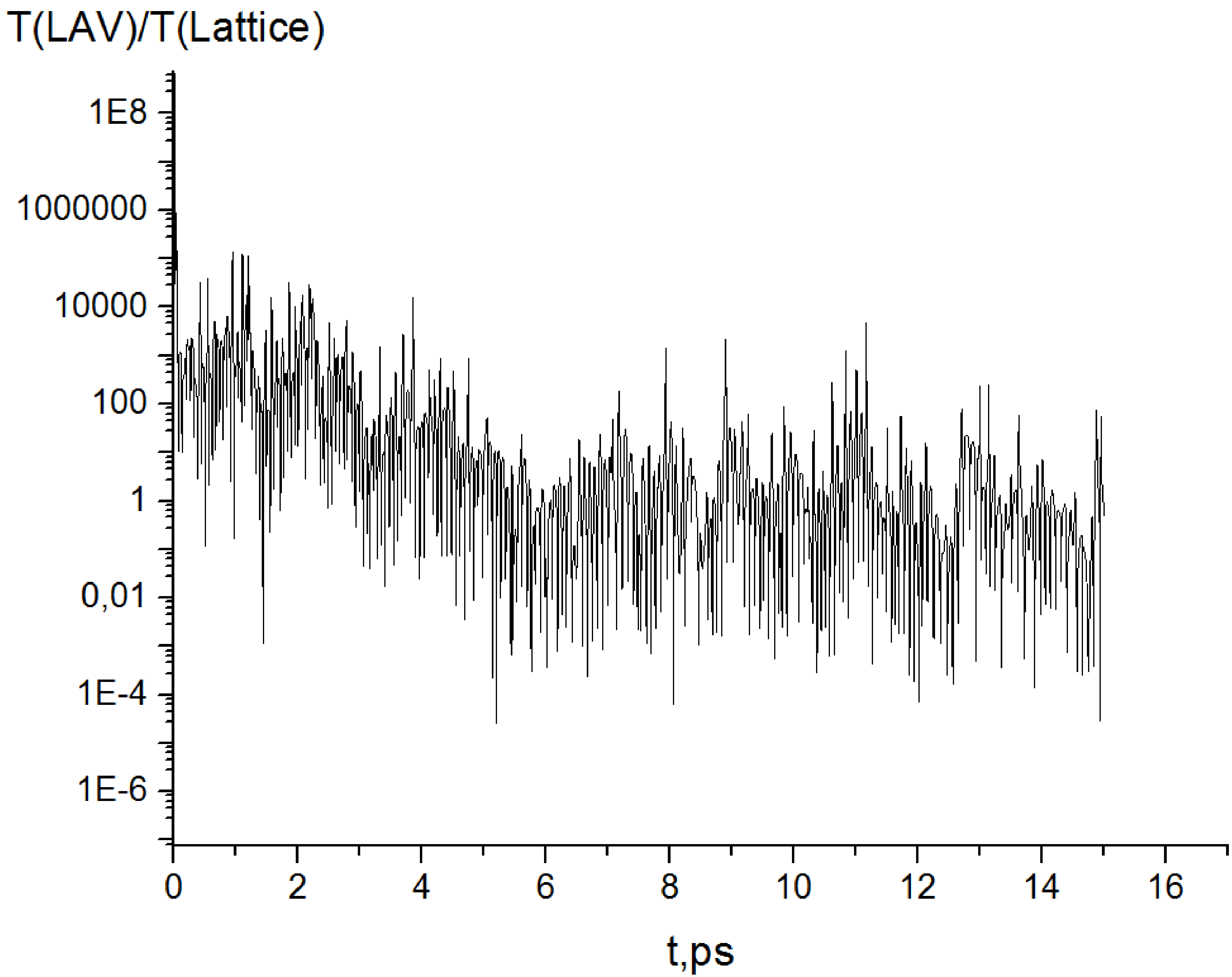

# DB effect (1): peiodic in time modulation of the potential barrier height

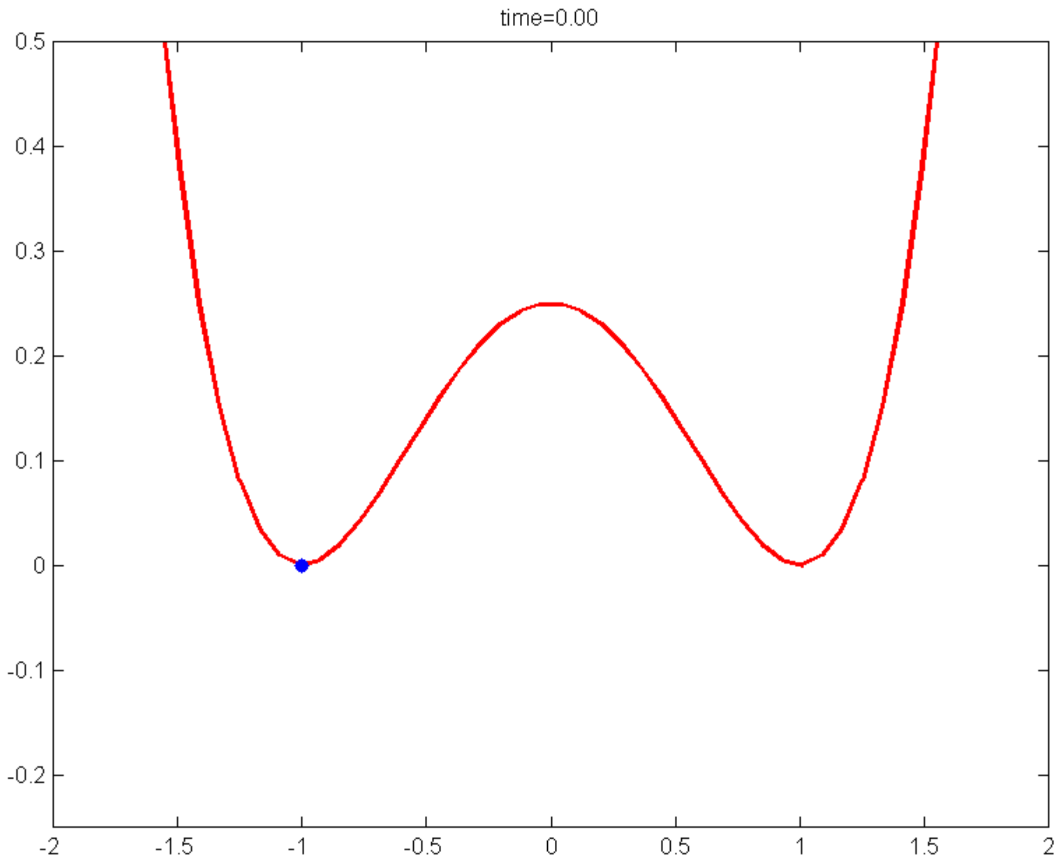

# *Reaction-rate theory with account of the crystal anharmonicity*

**Dubinko, Selyshchev, Archilla, Phys. Rev. E. (2011)**

$$R_K = \frac{\omega_0}{2\pi}\exp\left[-E_0/k_B T\right]$$ <= Kramers rate

$$U(x,t) = U(x) - (V \cdot x/x_m)\cos(\Omega t)$$

Kramers rate is amplified by:

$$I_0\left(V_m/k_B T\right)$$ - Bessel function

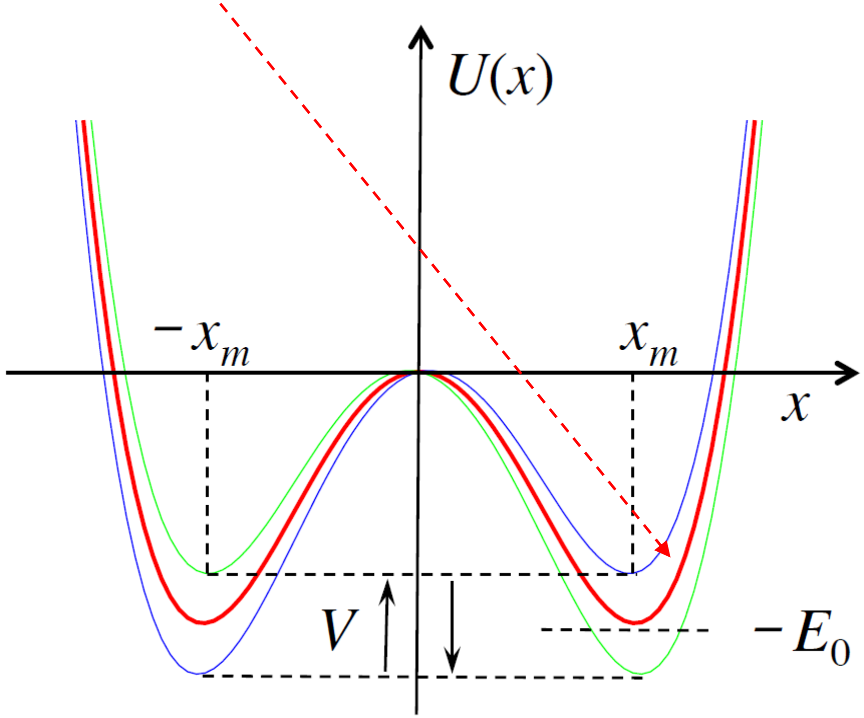


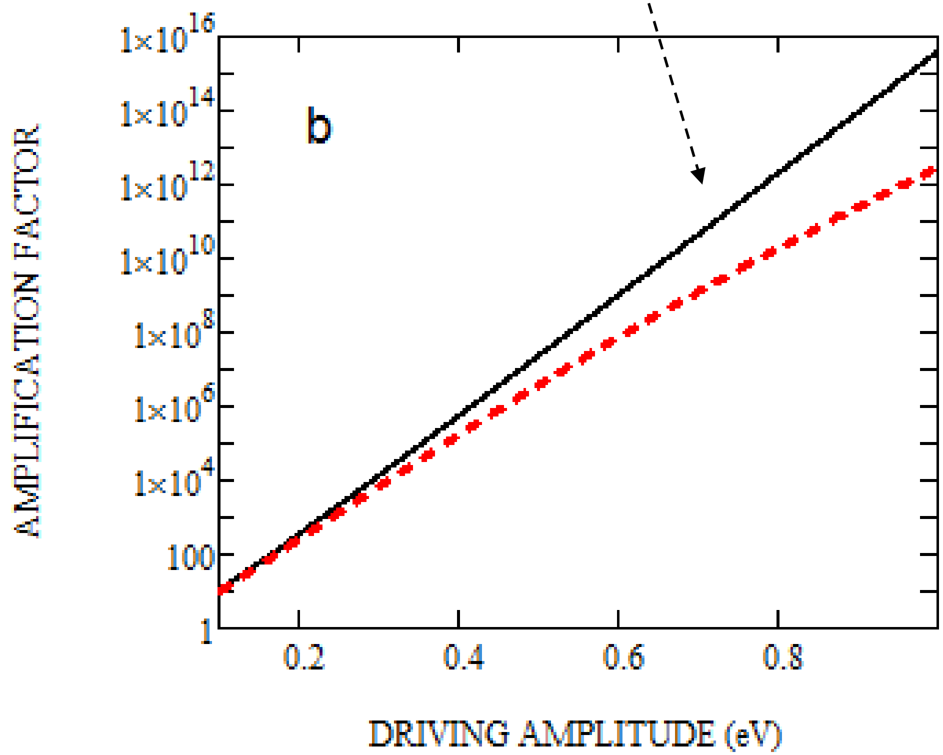

# Low temperature reconstructive transformation of muscovite

$K_2[Si_6Al_2]^{IV}[Al_4]^{VI}O_{20}(OH)_4$

Disilicate of Lutetium
$Lu_2Si_2O_7$

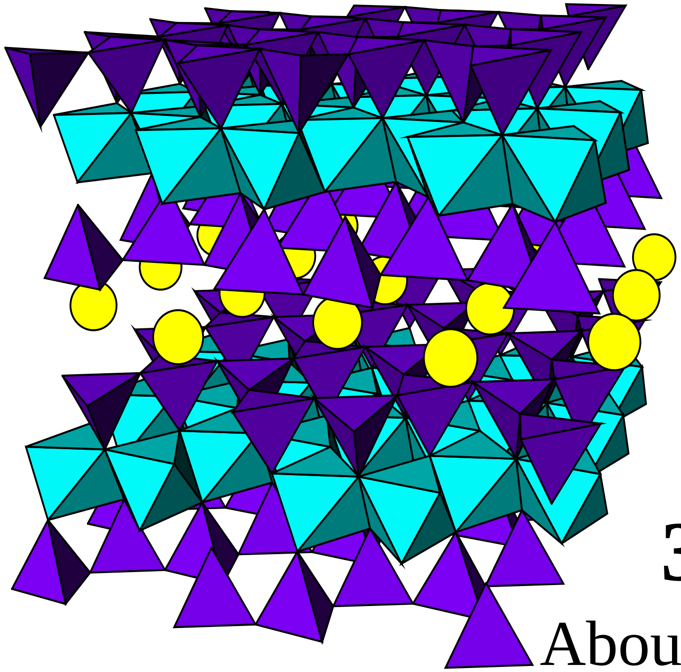

$E_a > 1$ eV

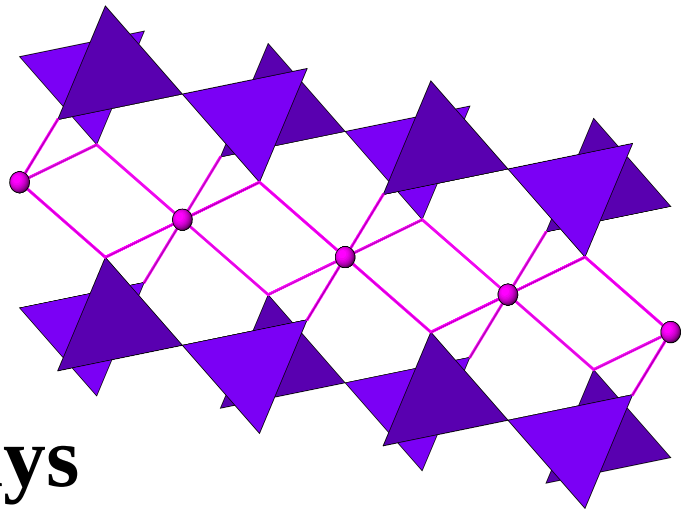

**300° C, 3 days**

About 36% of muscovite is transformed, which is
$10^4$ - $10^5$ times faster than by **Arrhenius law:**

○ $K^+$

**At T= 1000° C, 3 days**
**At T = 300° C, $10^3$ years**

⟺ $\dot{R}_K = \nu \exp(-E_a/k_b T)$

# Transformation rate of muscovite with account of DB statistics Dubinko et al (2011)

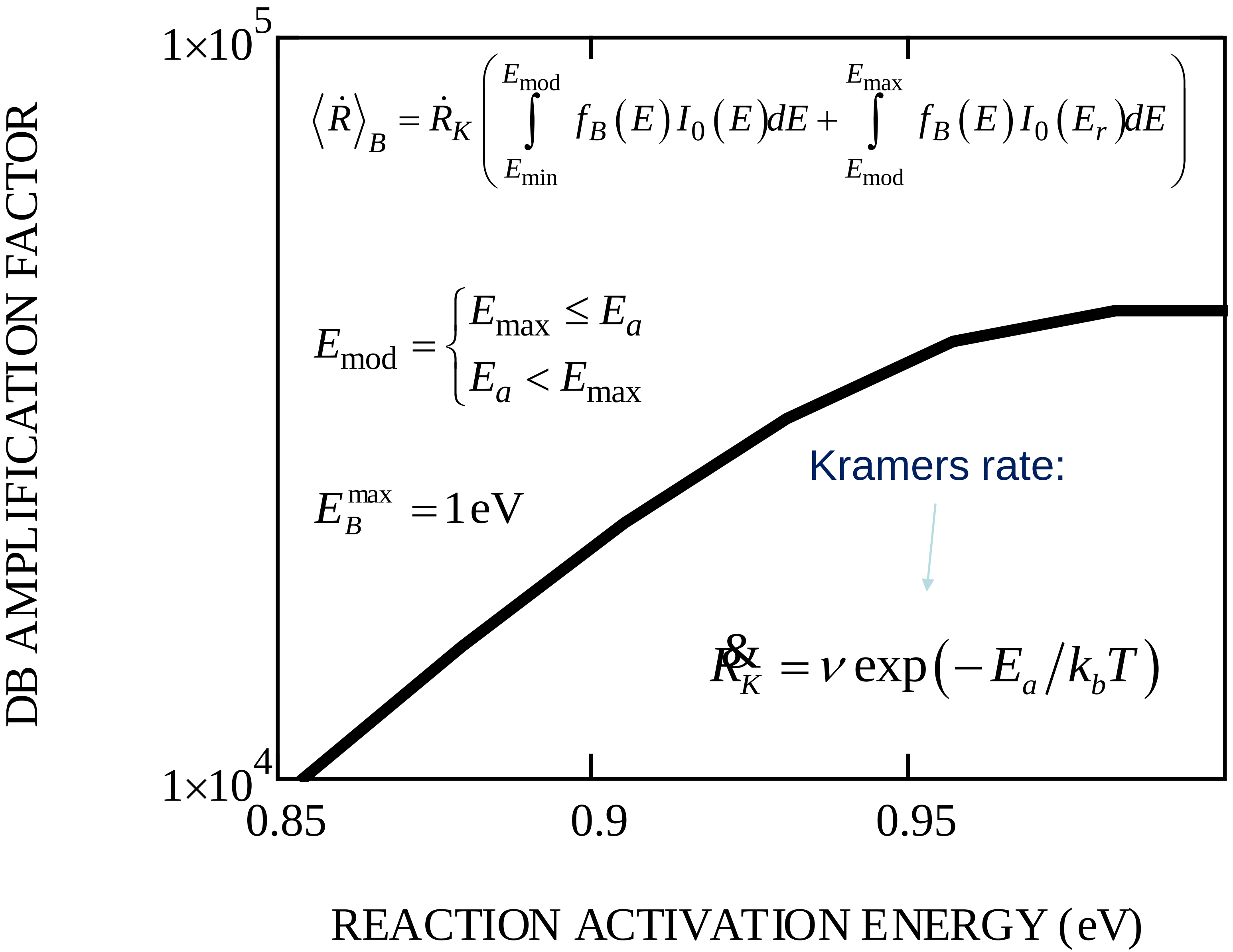

**How extend this concept to include**

**Quantum effects, Tunneling ?**

# **Tunneling:** Numerical solution of **Schrödinger equation**

Stationary: $t_{Kramers}$~$10^5$ cycles at $\mathbf{V_{barrier}=12E_0}$

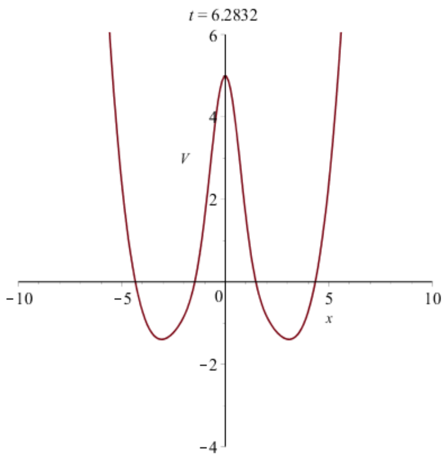


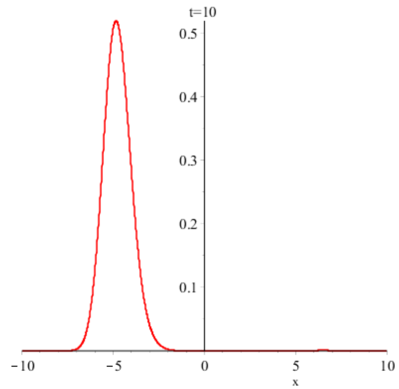


10 cycles

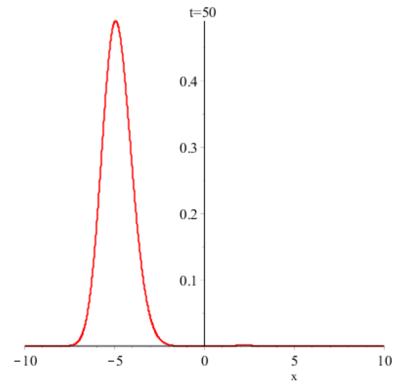


50 cycles

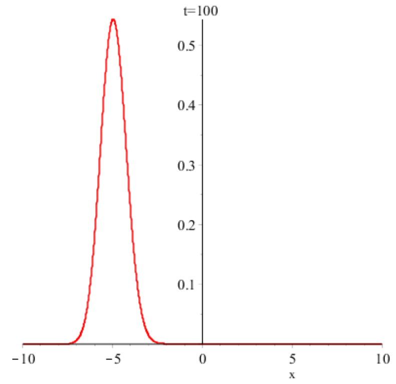


100 cycles

Time-periodically driven: $\mathbf{\Omega = 1.5\ \omega_0\ ,\ g = 0.2}$

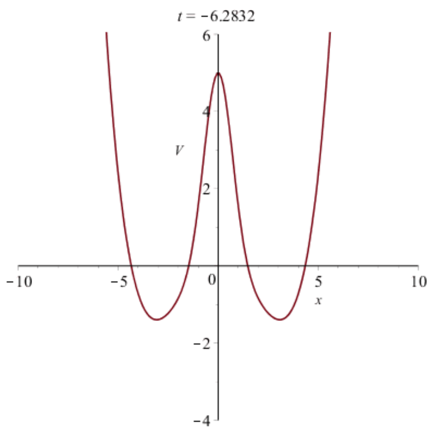


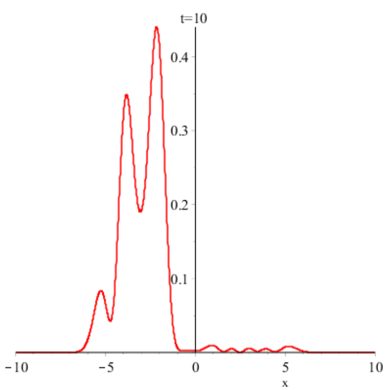


10 cycles

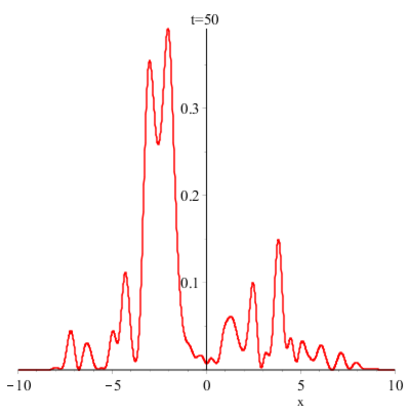


50 cycles

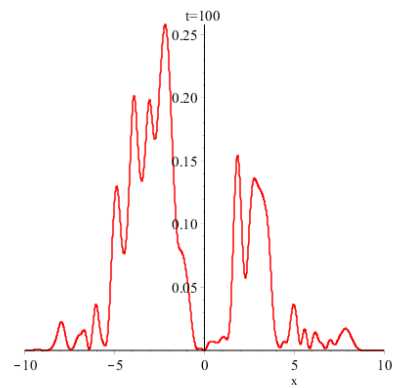


100 cycles

**Tunneling as a classical escape rate induced by the vacuum zero-point radiation**, A.J. Faria, H.M. Franca, R.C. Sponchiado Foundations of Physics (2006)

The Kramers theory is extended in order to take into account both the action of the thermal and zero-point oscillation (ZPO) energy.

$$R_K = \frac{\omega_0}{2\pi} \exp\left[-E_0 / D(T)\right]$$

$$D(T) = E_{ZPO} \coth\left(E_{ZPO}/k_B T\right) \approx \begin{cases} E_{ZPO}, & T \to 0 \\ k_B T, & T \gg E_{ZPO}/k_B \end{cases}$$

T – temperature is a measure of *thermal* noise strength

$$E_{ZPO} = \frac{\hbar\omega_0}{2}$$

- ZPO energy is a measure of *quantum* noise strength

When we heat the system we increase temperature, i.e. we increase the *thermal* noise strength

Can we increase the *quantum* noise strength, i.e. ZPO energy?

# Stationary harmonic potential

$$\langle E \rangle_n = \hbar\omega_0\left(n + \frac{1}{2}\right)$$

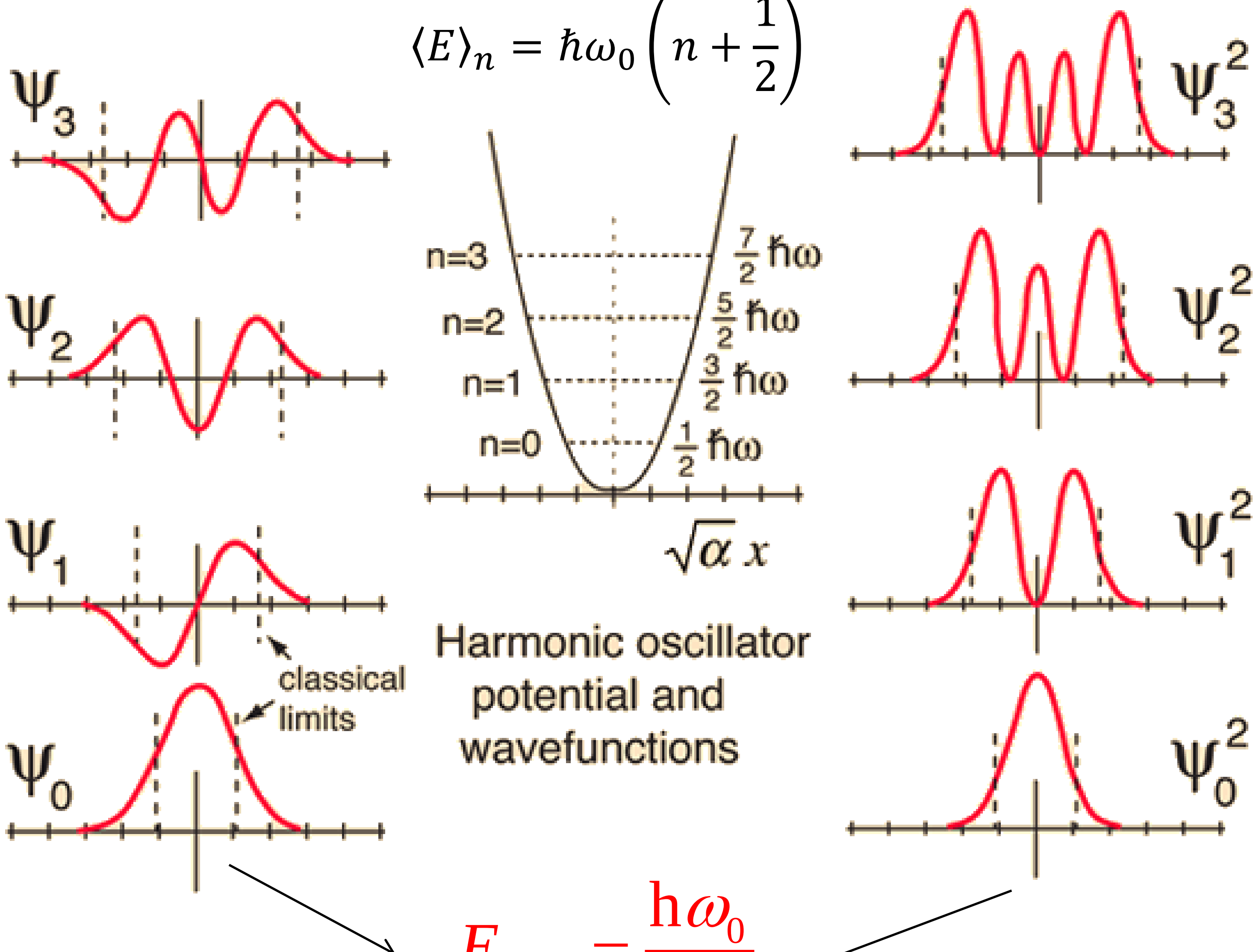


$$E_{ZPO} = \frac{h\omega_0}{2}$$

## Time-periodic modulation of the double-well shape changes (i) eigenfrequency and (ii) position of the wells

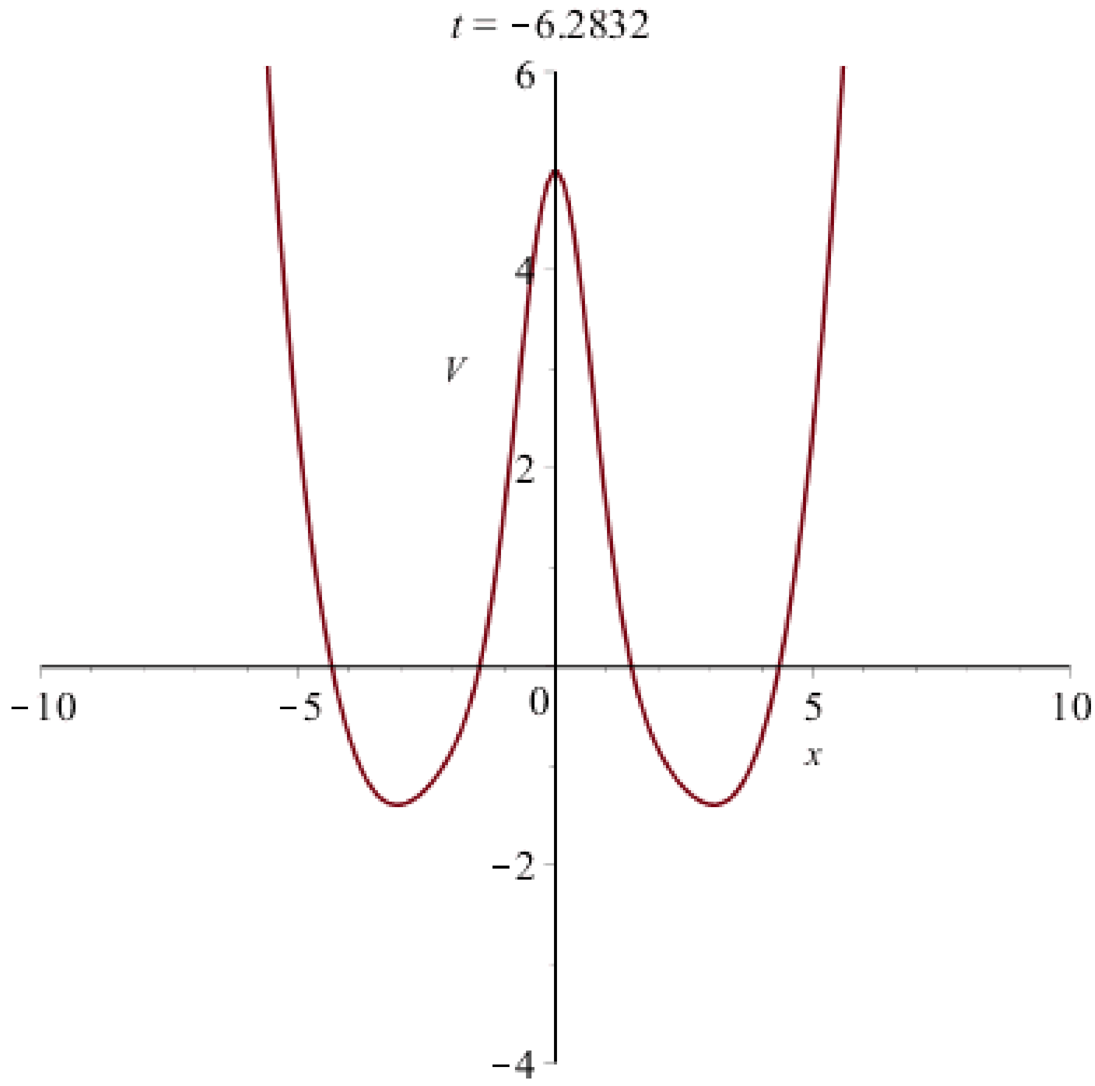

# Parametric resonance with **time-periodic eigenfrequency Ω = 2ω₀**

$$i\hbar \frac{\partial \psi}{\partial t} = -\frac{\hbar^2}{2m}\frac{\partial^2 \psi}{\partial x^2} + \frac{m\omega^2(t)}{2}x^2\psi$$

**Schrödinger equation**

$$\psi(x_0, t_0 = 0) = \frac{1}{\sqrt[4]{2\pi\sigma_0}}\exp\left(-\frac{x_0^2}{4\sigma_0}\right)$$

Initial Gaussian packet $\sigma_0 = \frac{\hbar}{2m\omega_0}$

**Parametric regime Ω = 2ω₀:**

$$\ddot{x} + \omega_0^2\left[1 - g\cos(2\omega_0 t)\right]x = 0$$

g << 1 – modulation amplitude

$$\sigma_x(t) = \sigma_0 \cosh\left(\frac{g\omega_0 t}{2}\right)\left[1 + \tanh\left(\frac{g\omega_0 t}{2}\right)\sin(2\omega_0 t)\right]$$

dispersion

**ZPO energy:**

$$E_{ZPO}(t) = \frac{\hbar\omega_0}{2}\cosh\frac{g\omega_0 t}{2}$$

**ZPO amplitude:**

$$\Lambda_{ZPO}(t) = \sqrt{\frac{\hbar}{2m\omega_0}\cosh\frac{g\omega_0 t}{2}}$$

# Non-stationary harmonic potential with **time-periodic eigenfrequency** $\Omega = 2\omega_0$

$$\Lambda_{ZPO}(t) = \sqrt{\frac{\hbar}{2m\omega_0}\cosh\frac{g\omega_0 t}{2}}$$

$$E_{ZPO}(t) = \frac{\hbar\omega_0}{2}\cosh\frac{g\omega_0 t}{2}$$

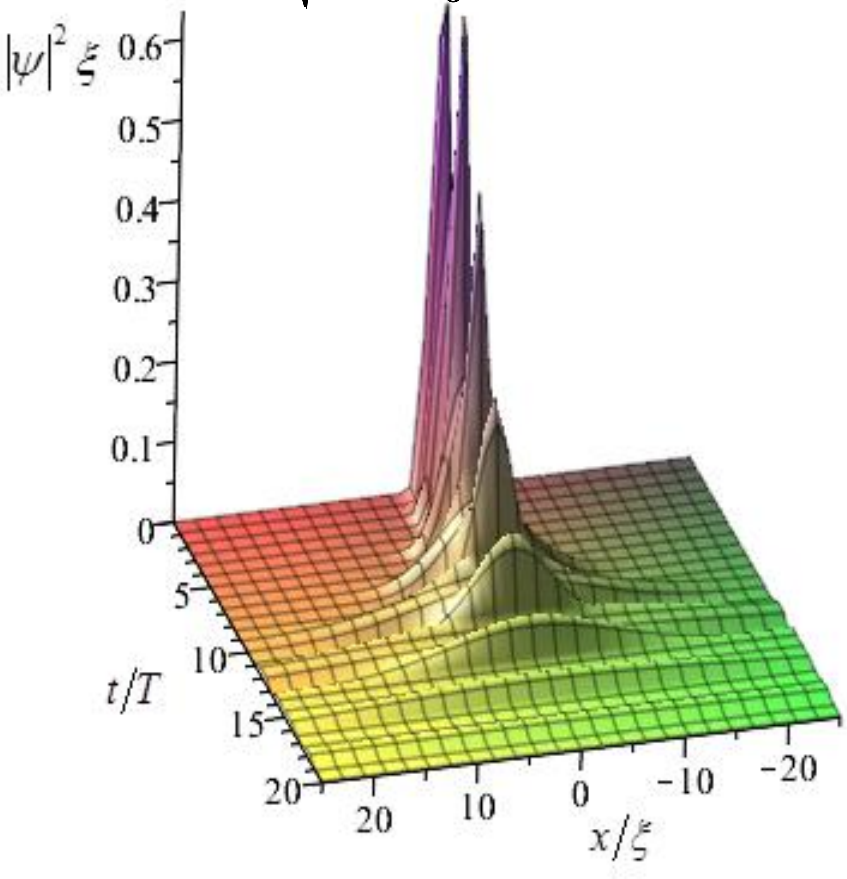


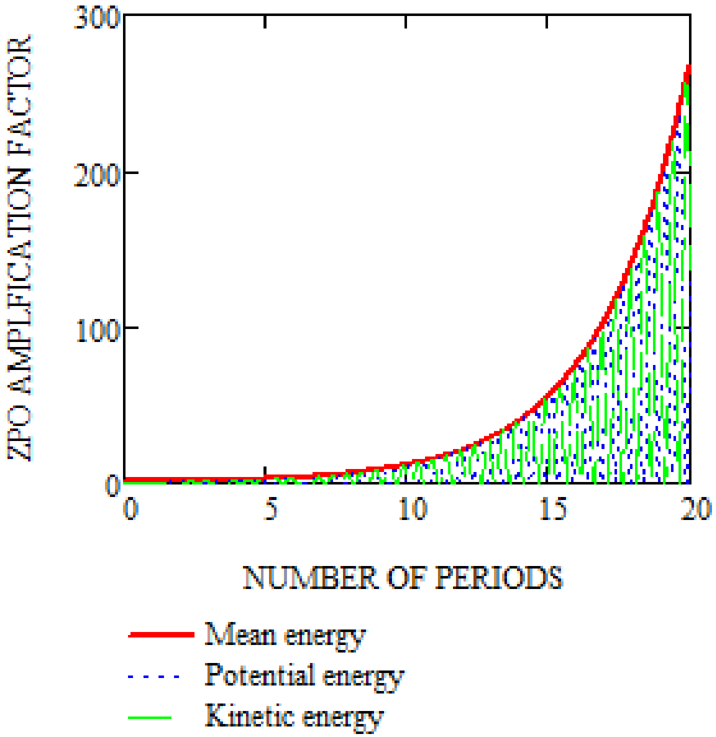

Escape rate in the modified Kramers theory with account of parametric driving of the **well eigenfrequency** **$\Omega = 2\omega_0$**

$E_0$ = 1 eV – the well depth; g=0.1 – the modulation amplitude

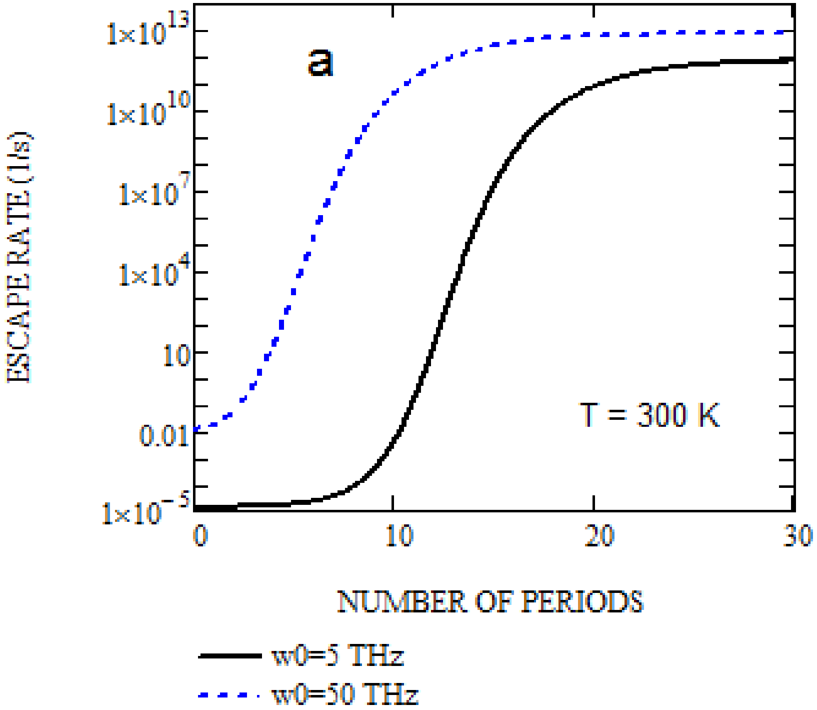


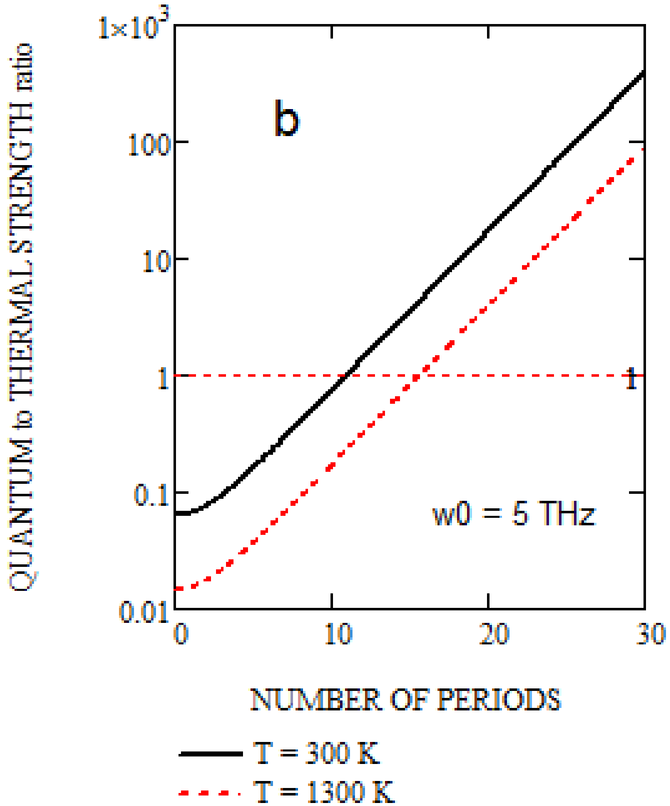

# Non-stationary harmonic potential with **time-periodic** shifting of the **well position at $\Omega = \omega_0$**

a

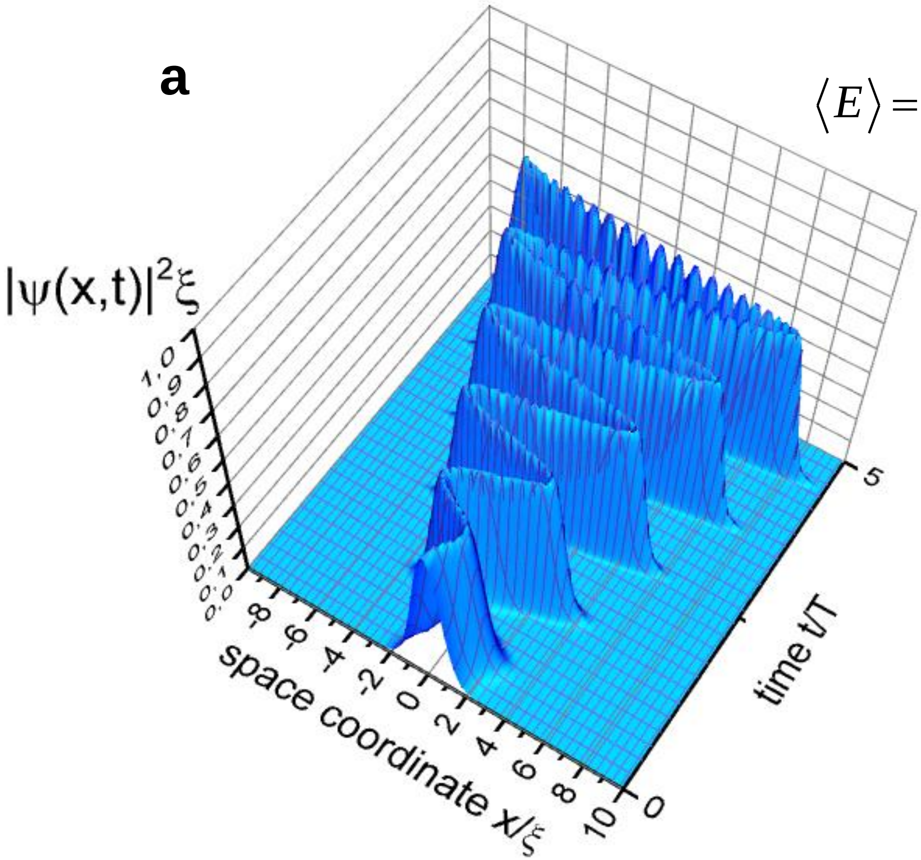


$$\langle E\rangle = \frac{h\omega_0}{2} + \frac{(g_A A_{ZPO})^2 m\omega_0^2}{8}\left[\omega_0^2 t^2 + \omega_0 t \sin 2\omega_0 t + \sin^2 \omega_0 t\right]$$

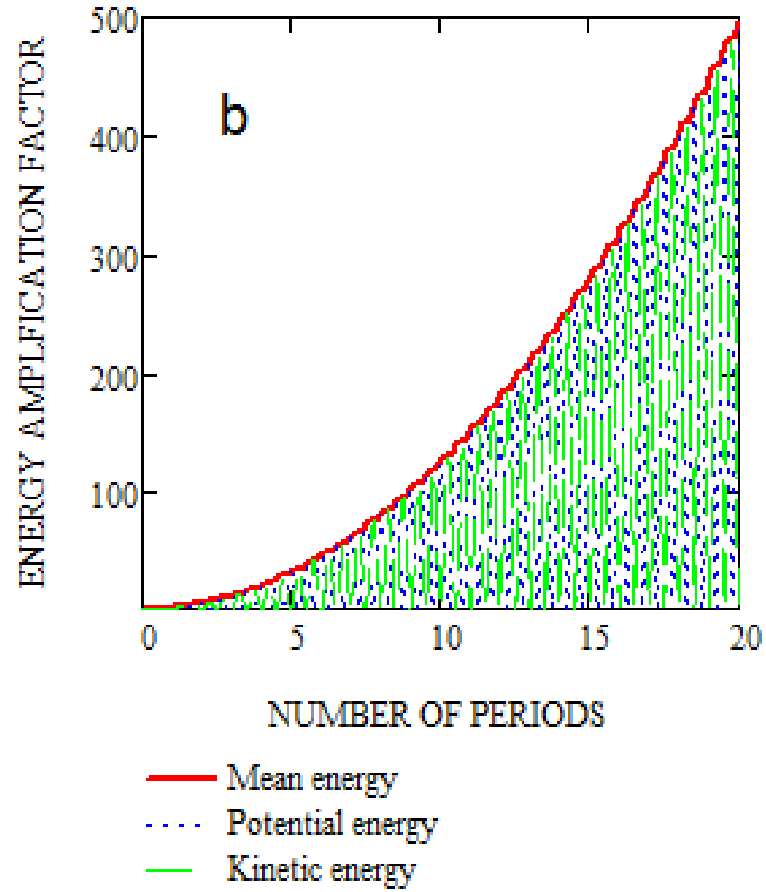


$$\lambda(t) = \frac{g_A A_{ZPO}}{2}\omega_0 t\left(\cos\omega_0 t - \frac{\sin\omega_0 t}{\omega_0 t}\right)$$

# Escape rate in the modified Kramers theory with account of parametric driving of the well **position** at **$\Omega = \omega_0$**

$$R_K = \frac{\omega_0}{2\pi}\exp\left[-\left(E_0 - \langle E\rangle\right)/D(T)\right] \qquad D(T) = \frac{\hbar\omega_0}{2}\coth\left(\hbar\omega_0/2k_BT\right)$$

$E_0$ = 1 eV – well depth; $g_A$ =0.5 – modulation amplitude

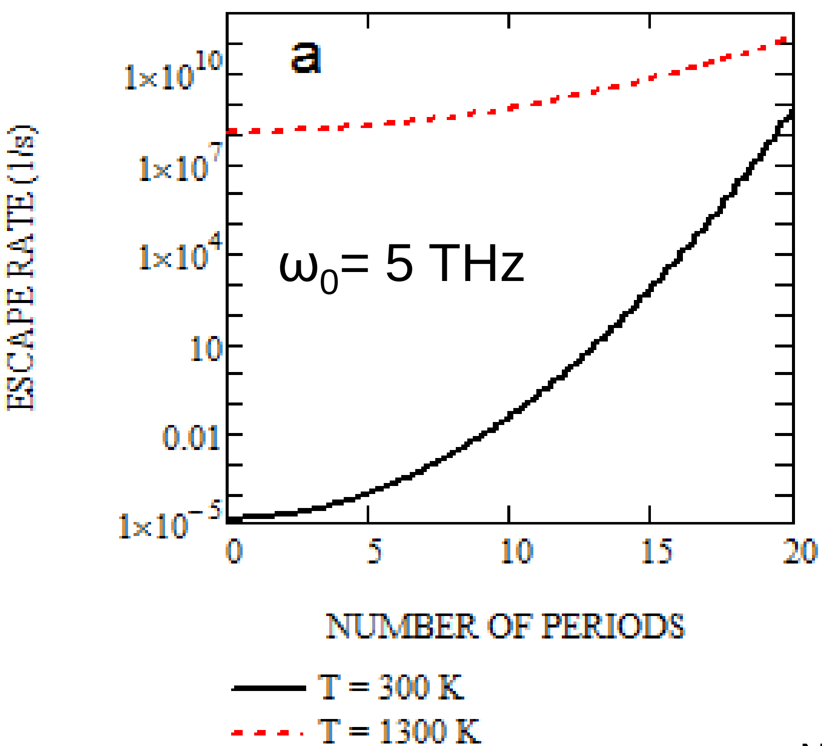


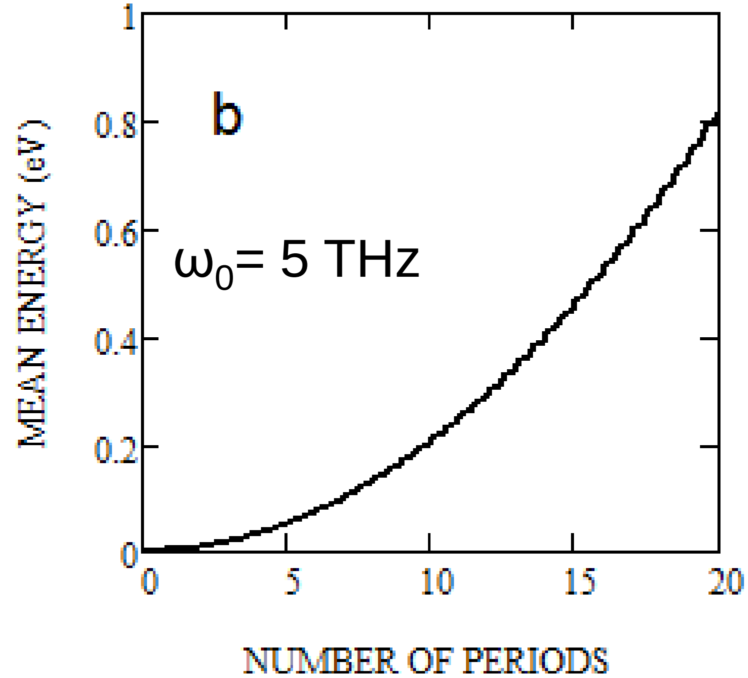


Nolineal 2016

# **Tunneling:** Numerical solution of **Schrödinger equation**

Stationary: $t_{Kramers}$~$10^5$ cycles at $\mathbf{V_{barrier}=12E_0}$

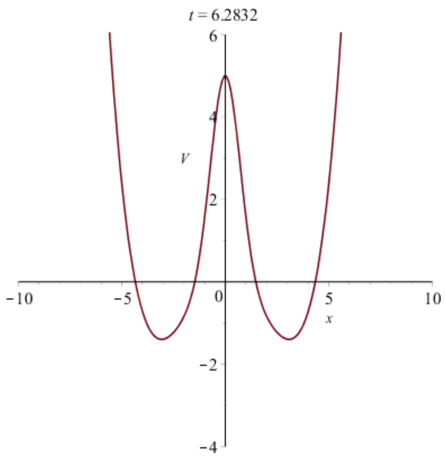


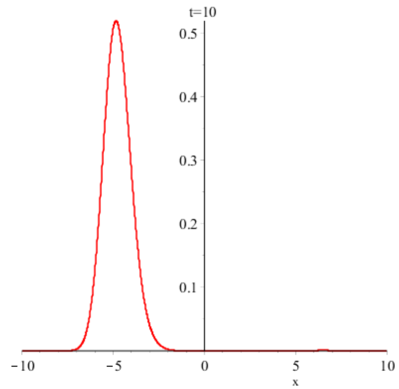


10 cycles

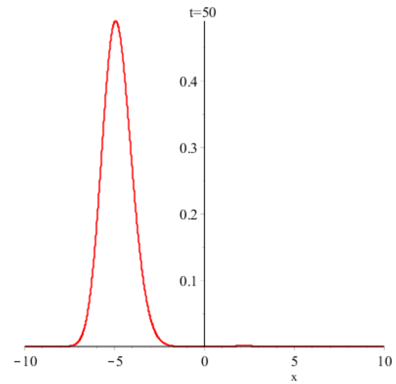


50 cycles

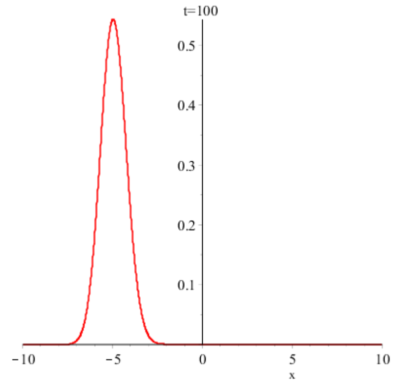


100 cycles

Time-periodically driven: $\mathbf{\Omega = 1.5\ \omega_0\ ,\ g = 0.2}$

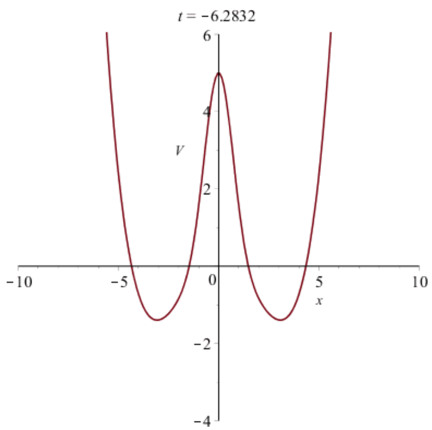


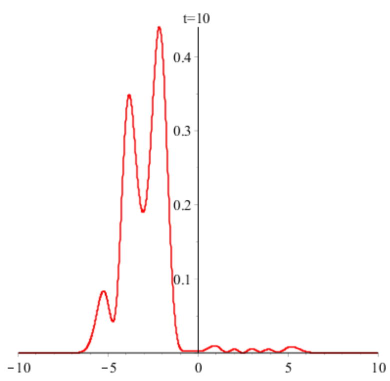


10 cycles

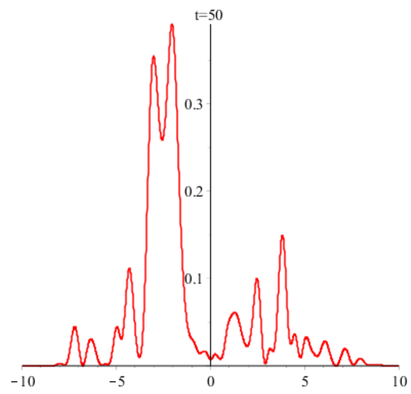


50 cycles

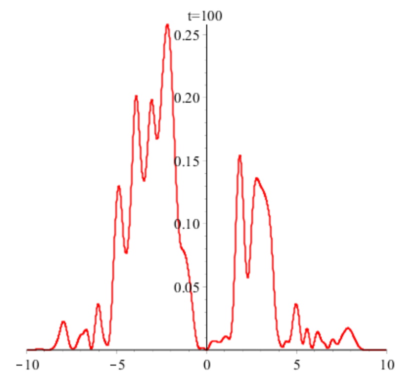


100 cycles

# DBs at finite T
# in diatomic crystals

# Gap DBs in NaCl type lattices, Dmitriev et al (2010)

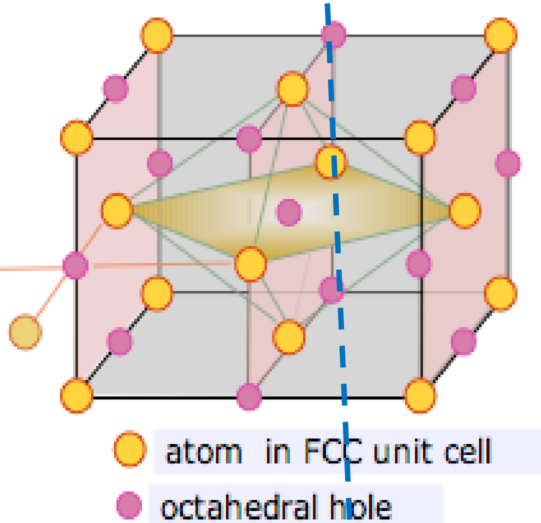


Phonon Gap

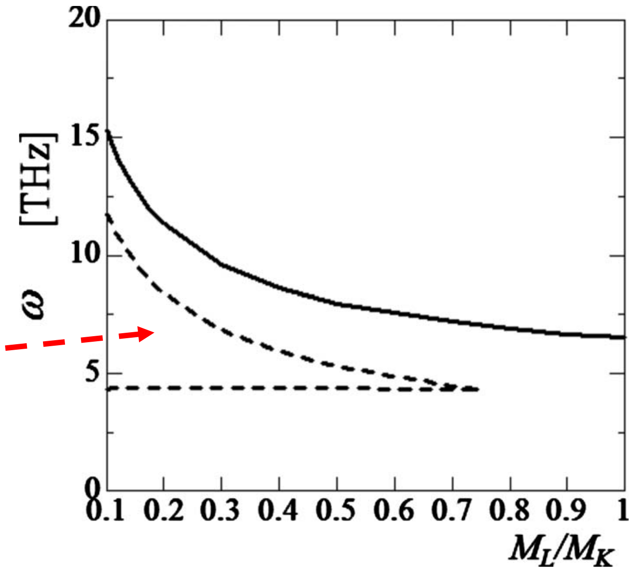


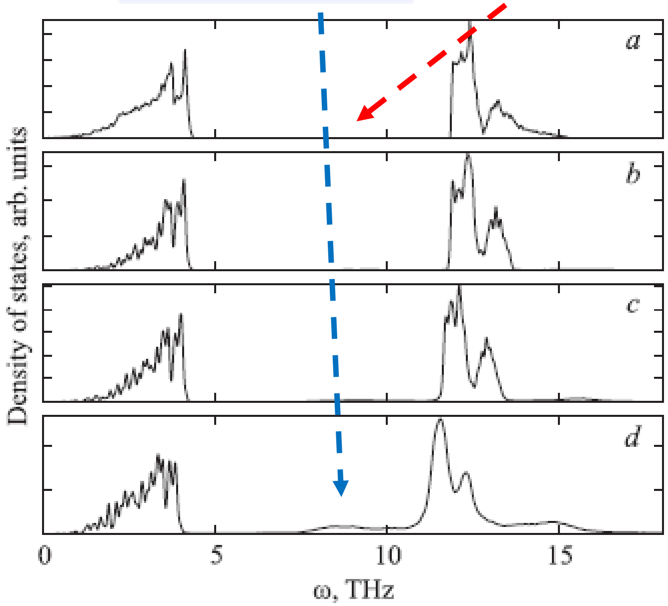


NaCl-type $M_H/M_L = 10$ at temperatures T = (a) 0, (b) 155, (c) 310, and (d) 620 K

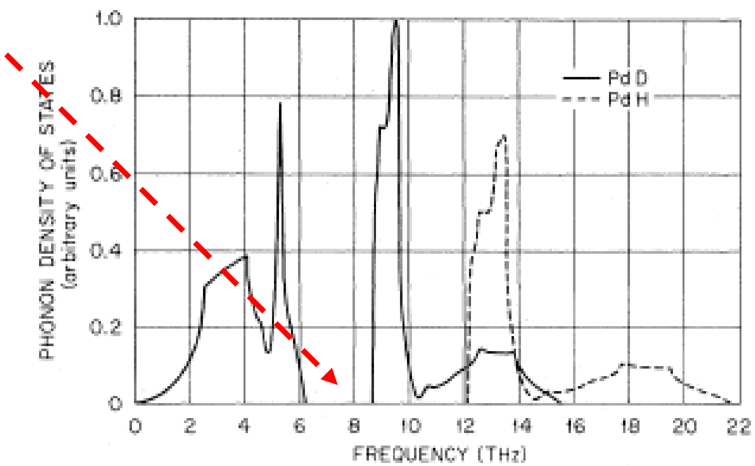


DOS for **$PdD_{0.63}$** and **$PdH_{0.63}$**: $M_H/M_L = 50; 100$
D pressure of 5 GPa and T=600 K

# MD modeling of LAVs in NiH and PdH crystals

# Visualization of the Pd(Ni)H fcc Lattice (NaCl type)

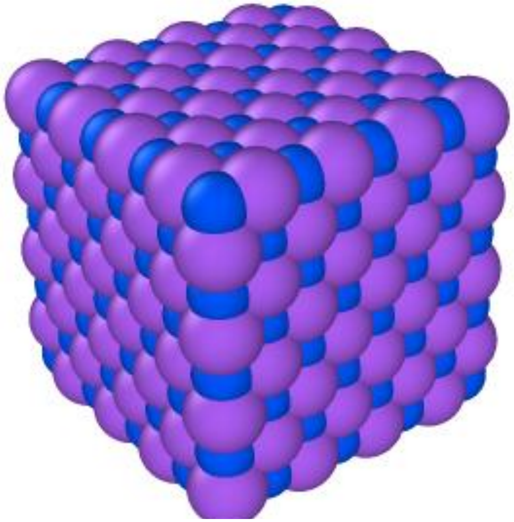

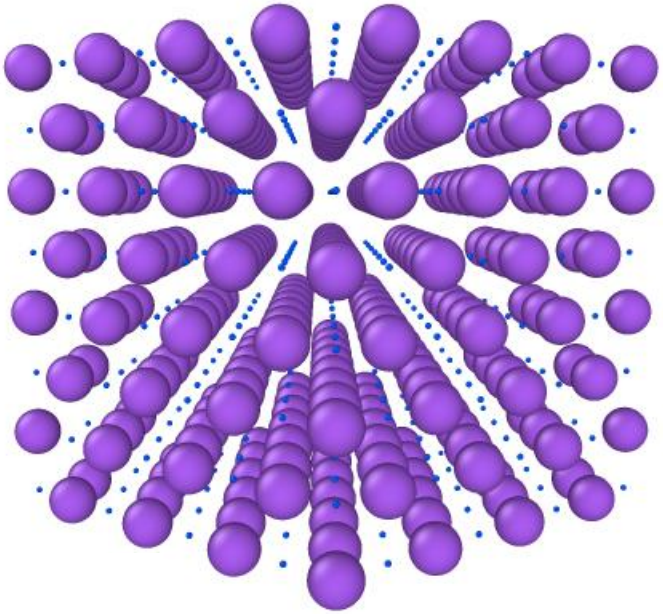

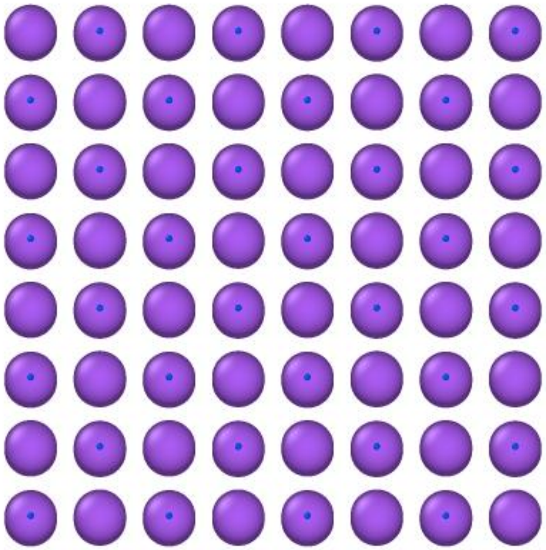

# NiH lattice

The following potential was used for Ni lattice modeling in **LAMMPS** package:

| Material | File with potential used | The link to the corresponding publication in the literature |
|---|---|---|
| NiH | NiAlH_jea.eam.alloy | see James E Angelo, Neville R Moody, Michael I Baskes"Trapping of hydrogen to lattice defects in nickel", Modelling andSimulation in Materials Science & Engineering, vol. 3, pp. 289-307 (1995) |

# Density Of States of NiH at 0 K

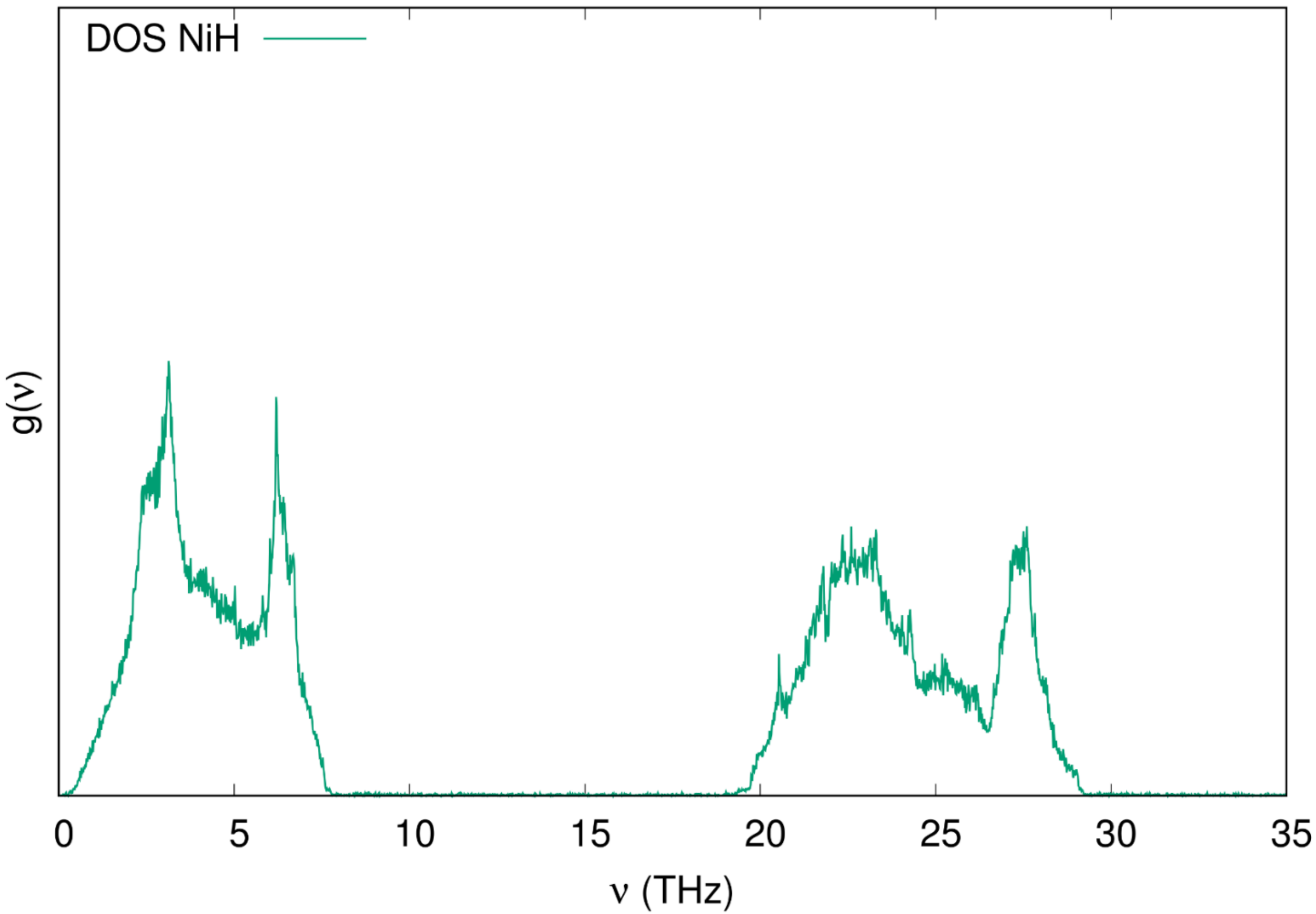

## 1 H atom displaced along[110] in NiH at T=0K

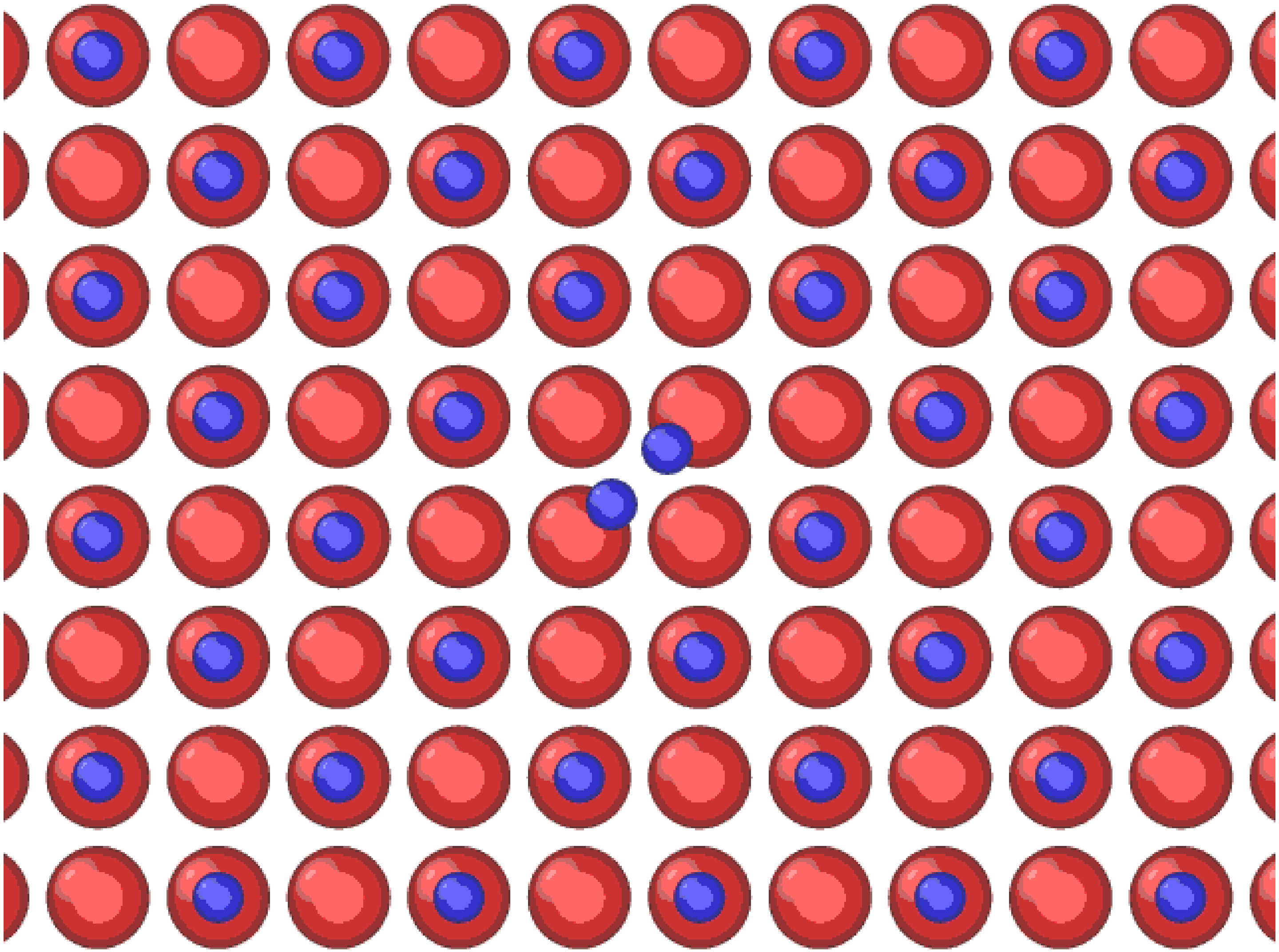

# 1 H atom displaced along <110> in NiH at T=0K

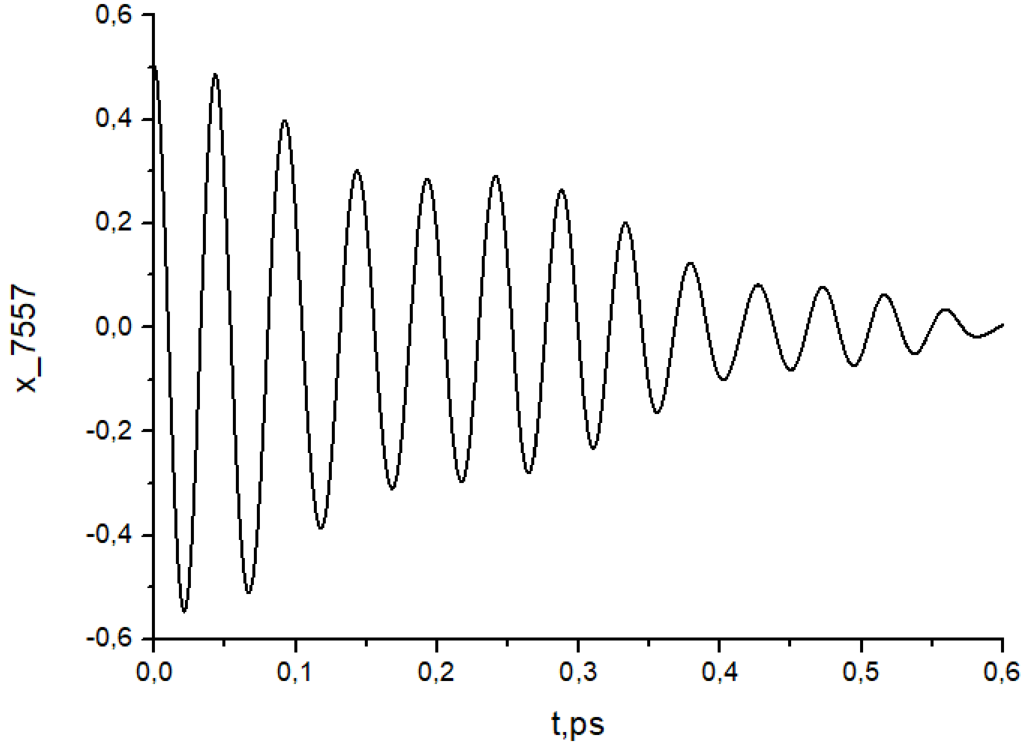


T=0.5 ps, Frequency = 20THz (**inside** the optical band)

# Discrete Breather in the 3d NiH Lattice at 0 K

## 1 atom H is displaced along <100> at 0.8 A. Initial velocity = 0.

**DB frequency= 29 THz**
**DB amplitude= 0.9A**
**Lattice constant= 3.5A**

$$\rho_i = \sum_j f_j(r_{ij})$$

$$E = \sum_{i<j} V_{ij}(r_{ij}) + \sum_i F_i(\rho)_i$$

The Embedded Atom Method has been used

**DB frequency lies near the upper edge of the phonon band**

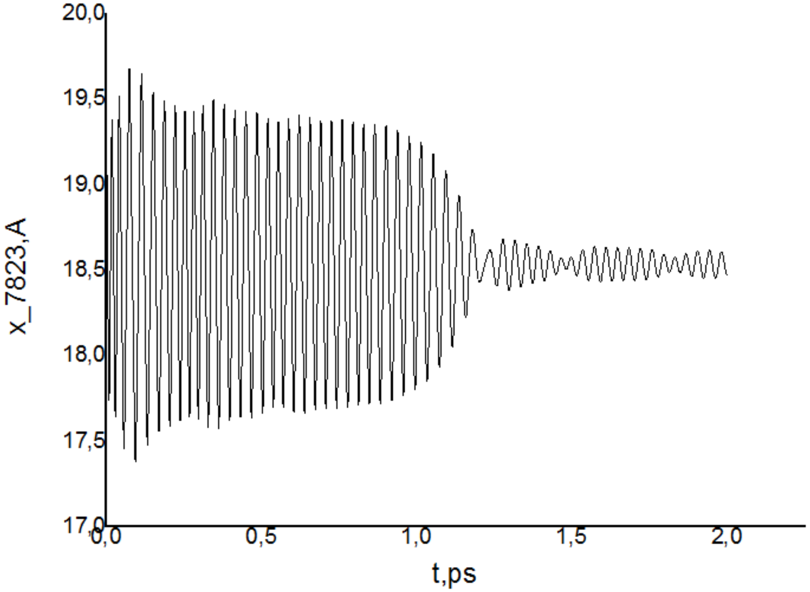


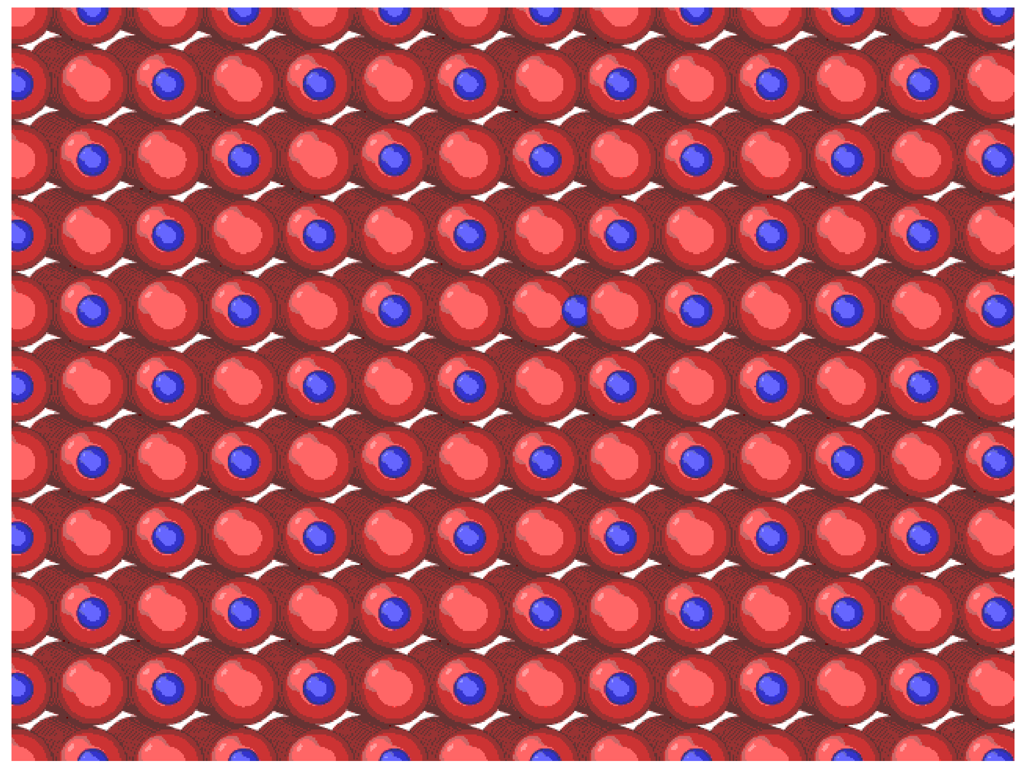

# 2 H atoms [100] and [-100] in NiH at T=0K

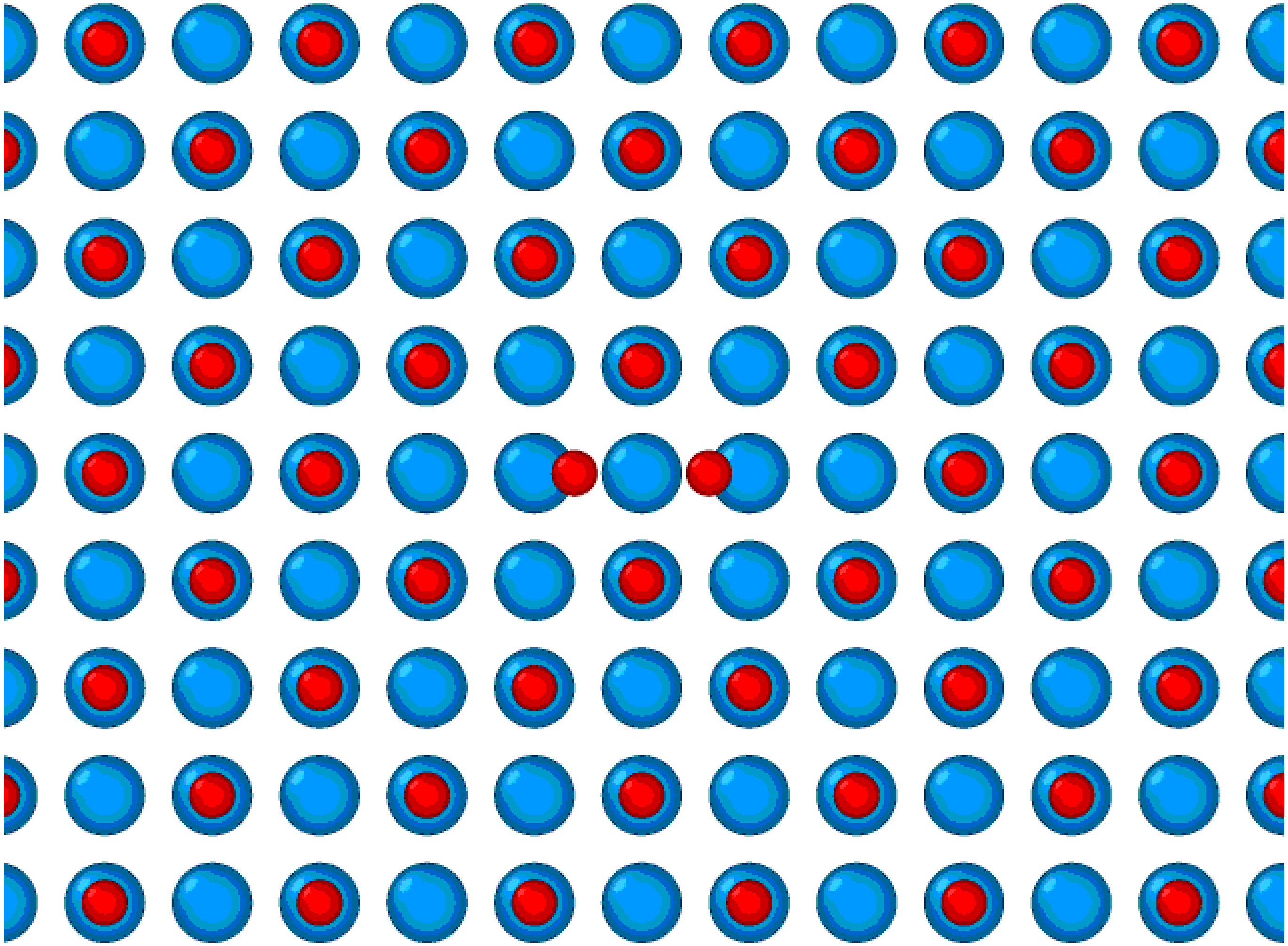

# 2 H atoms [100] and [-100] in NiH at T=0K

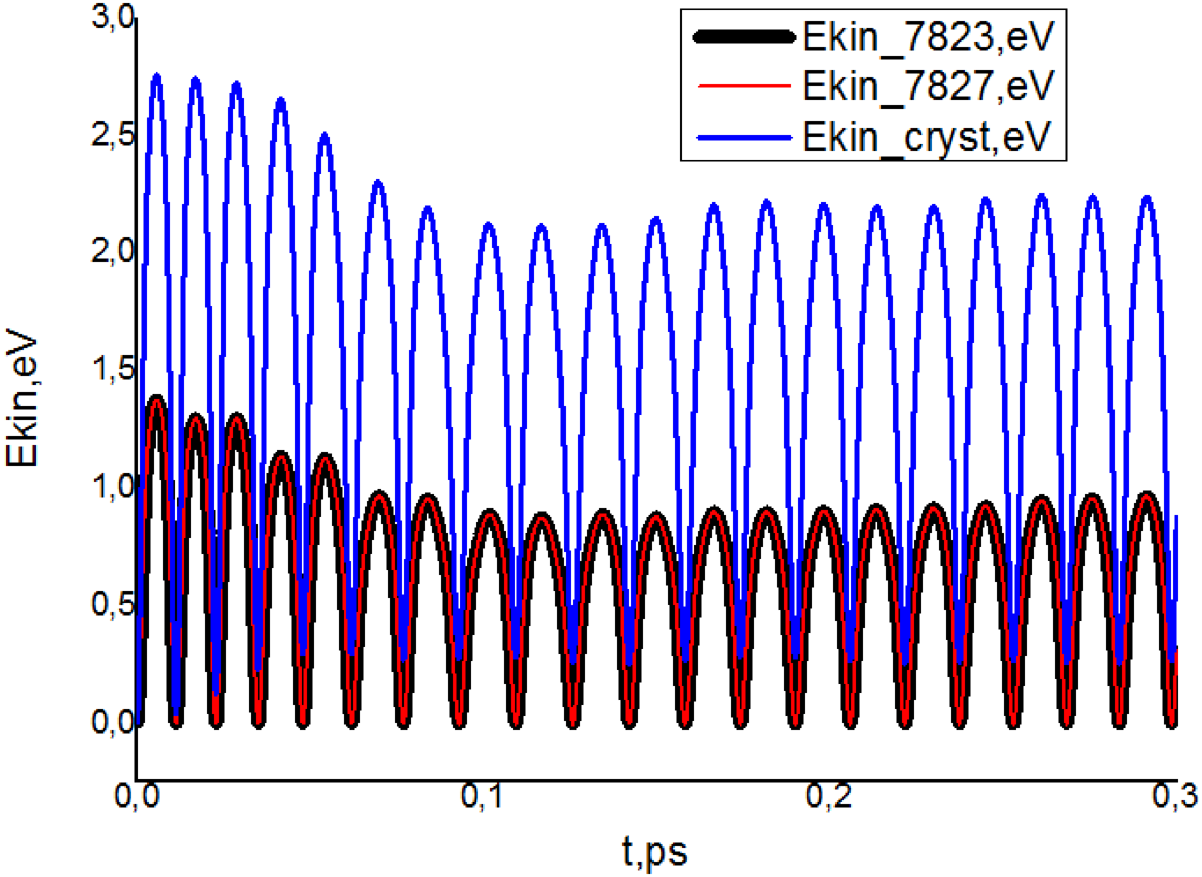

# 2 H atoms [100] and [-100] in NiH at T=0K

DB frequency = 33 THz **(above the optic band)**
DB amplitude = 0.8A
Lattice constant = 3.5A

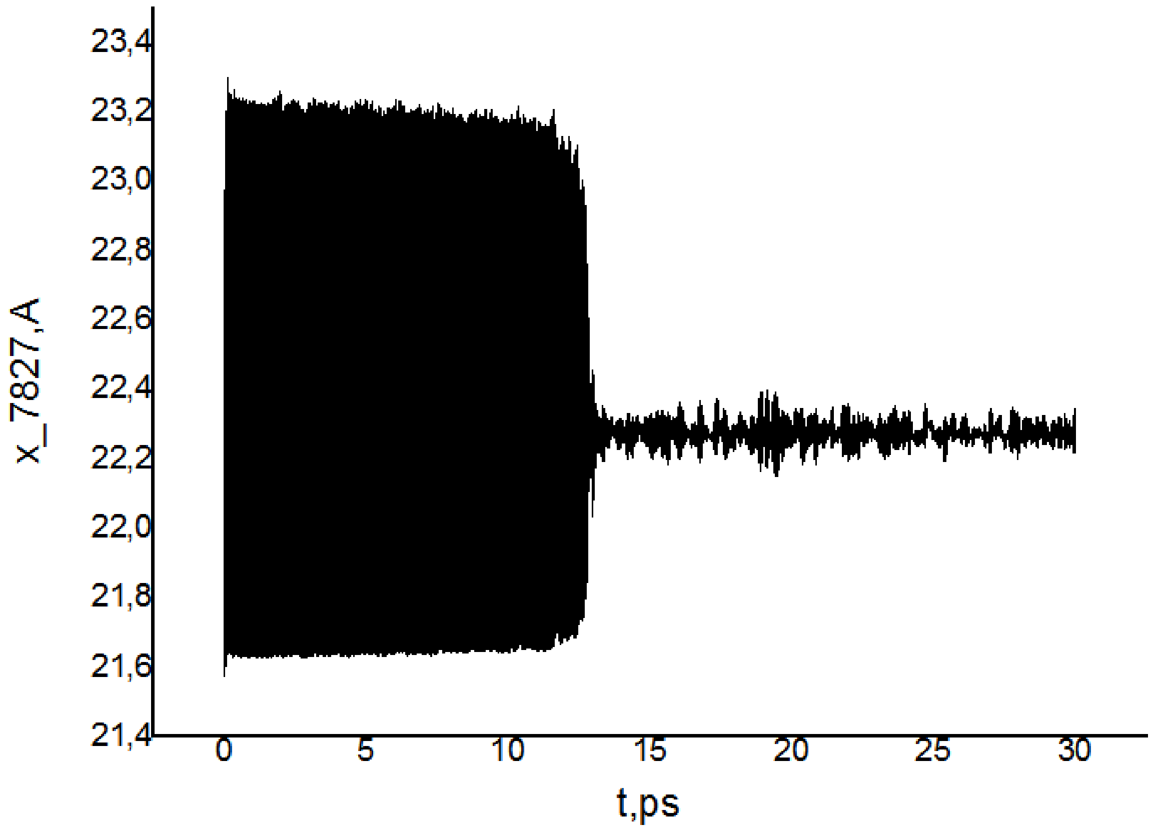

# Do DBs exist at finite T ?

# Visualization of the PdH fcc Lattice Oscillations at T=100 K

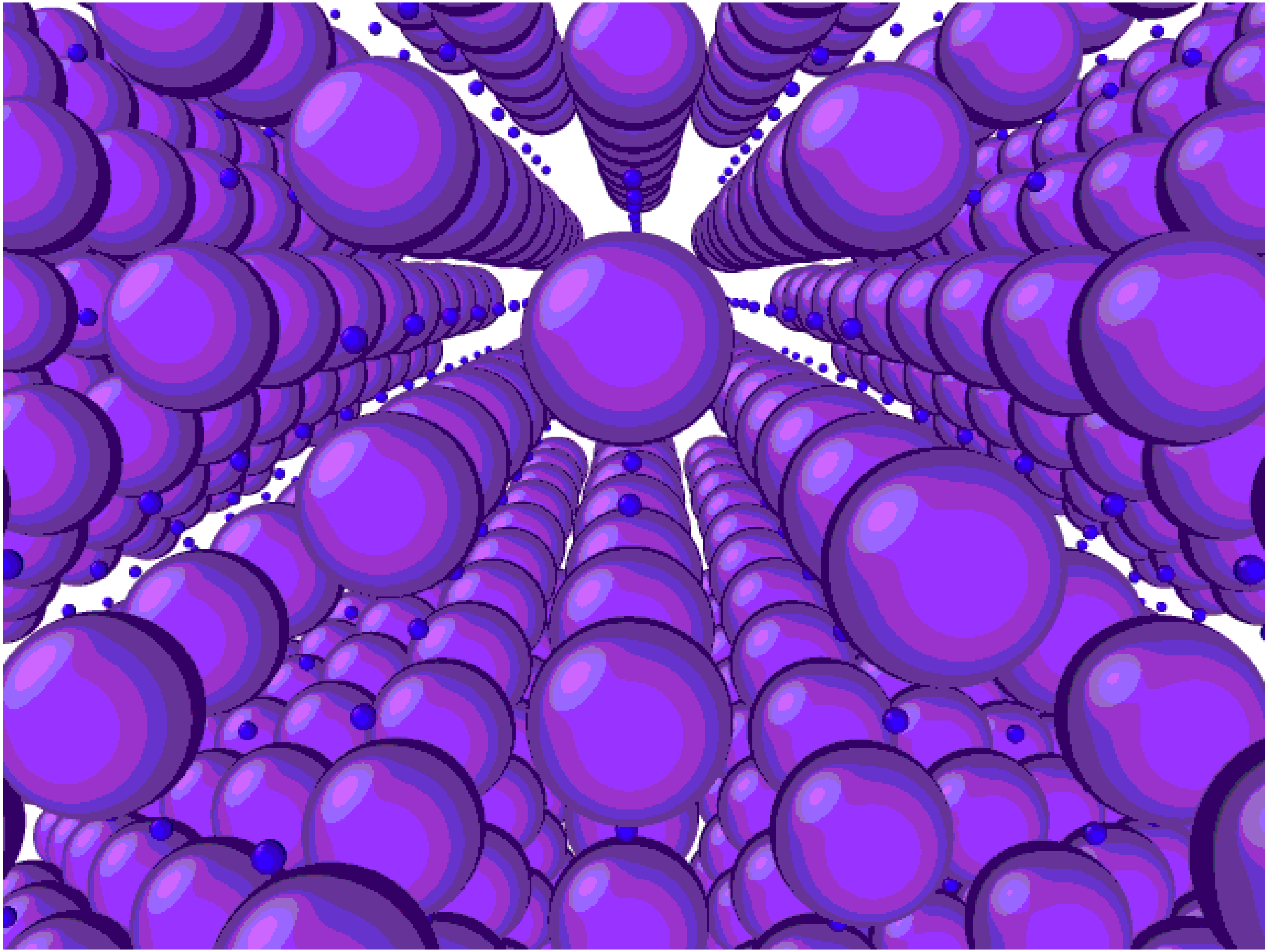

# Visualization of the PdH fcc Lattice Oscillations at T=1000K

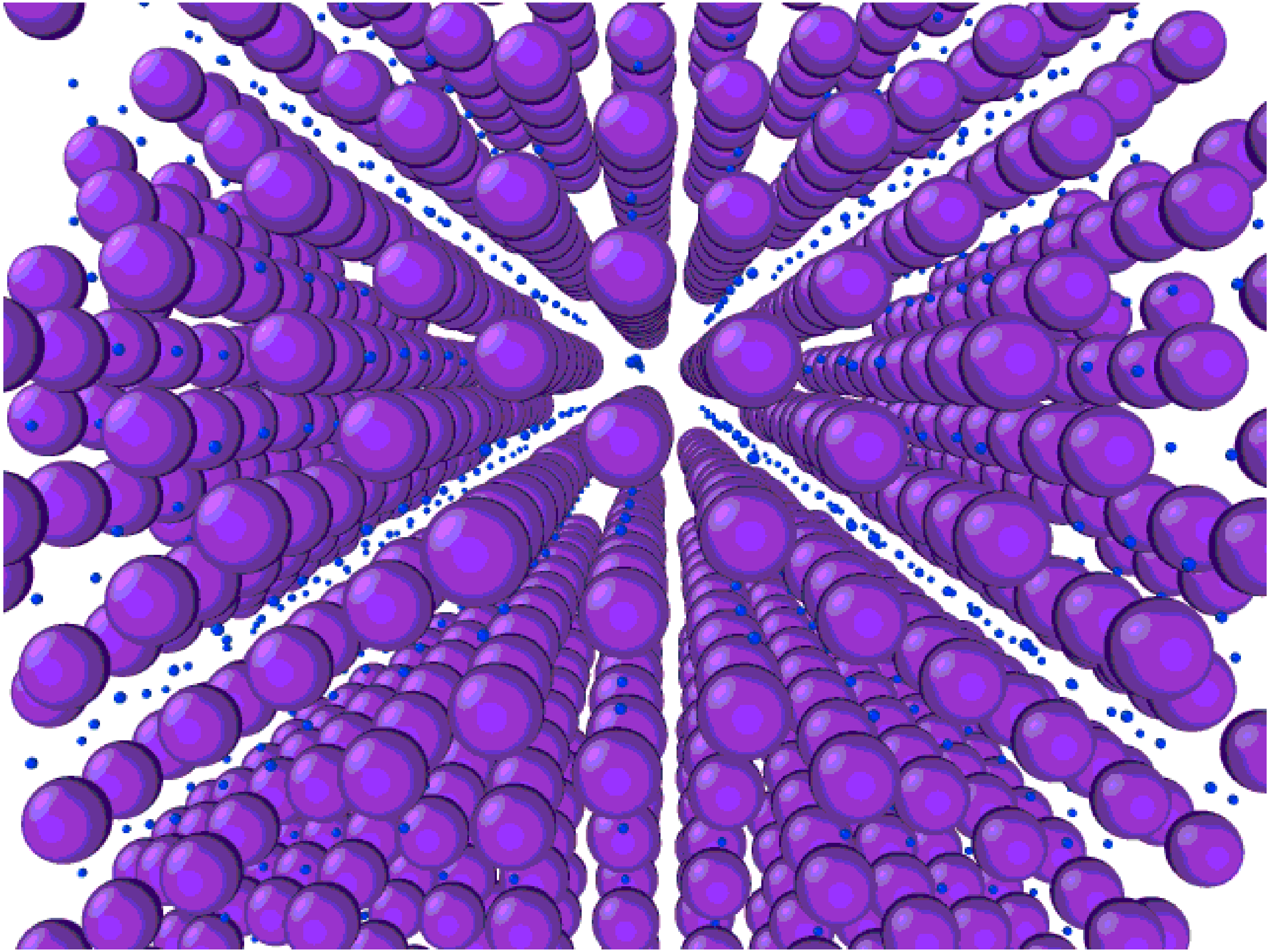

# Gap DBs in diatomic crystals at elevated temperatures

Hizhnyakov et al (2002), Dmitriev et al (2010)

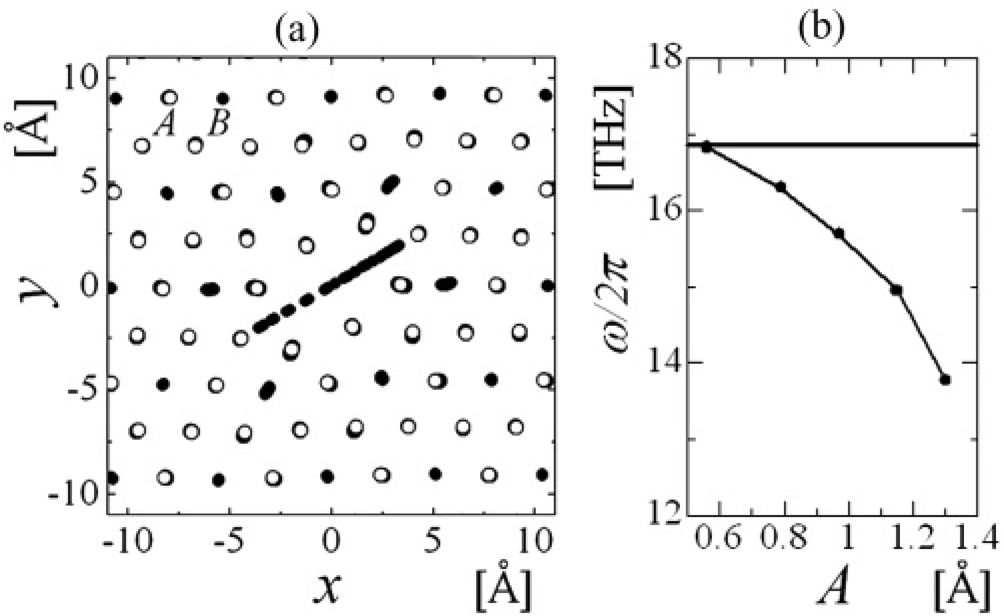


$K^*_{B,n}/\bar{K} \approx 5.1$

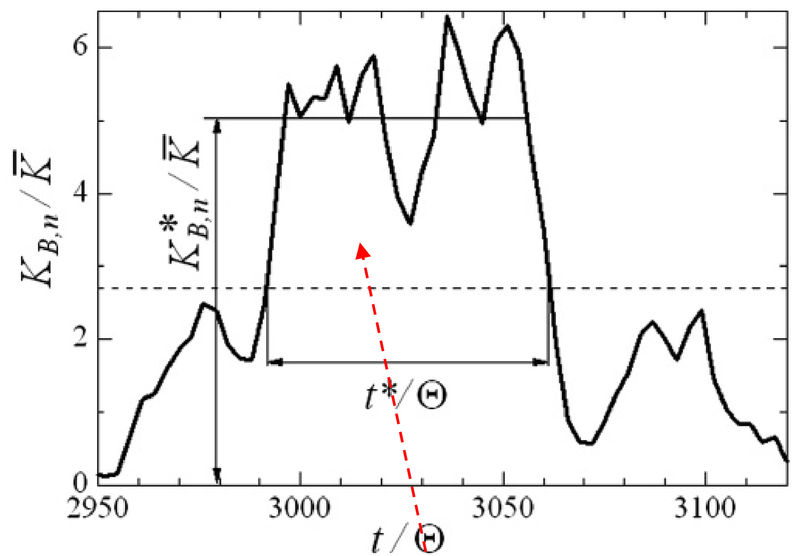


$A_3B$ type crystals $M_H/M_L = 10$

$t^*/\Theta \approx 70$ $\bar{K} = 0.1 eV \geq 1000 K$

In NaI and KI crystals Hizhnyakov et al has shown that DB amplitudes along <111> directions can be as high as 1 Å, and $t^*/\Theta \sim 10^4$

Lifetime and concentration of ***high-energy light atoms*** increase exponentially with increasing T

L. Kistanov, S. Dmitriev, Spontaneous excitation of discrete breathers in crystals with the structure of NaCl at elevated temperatures, FTT (2012)

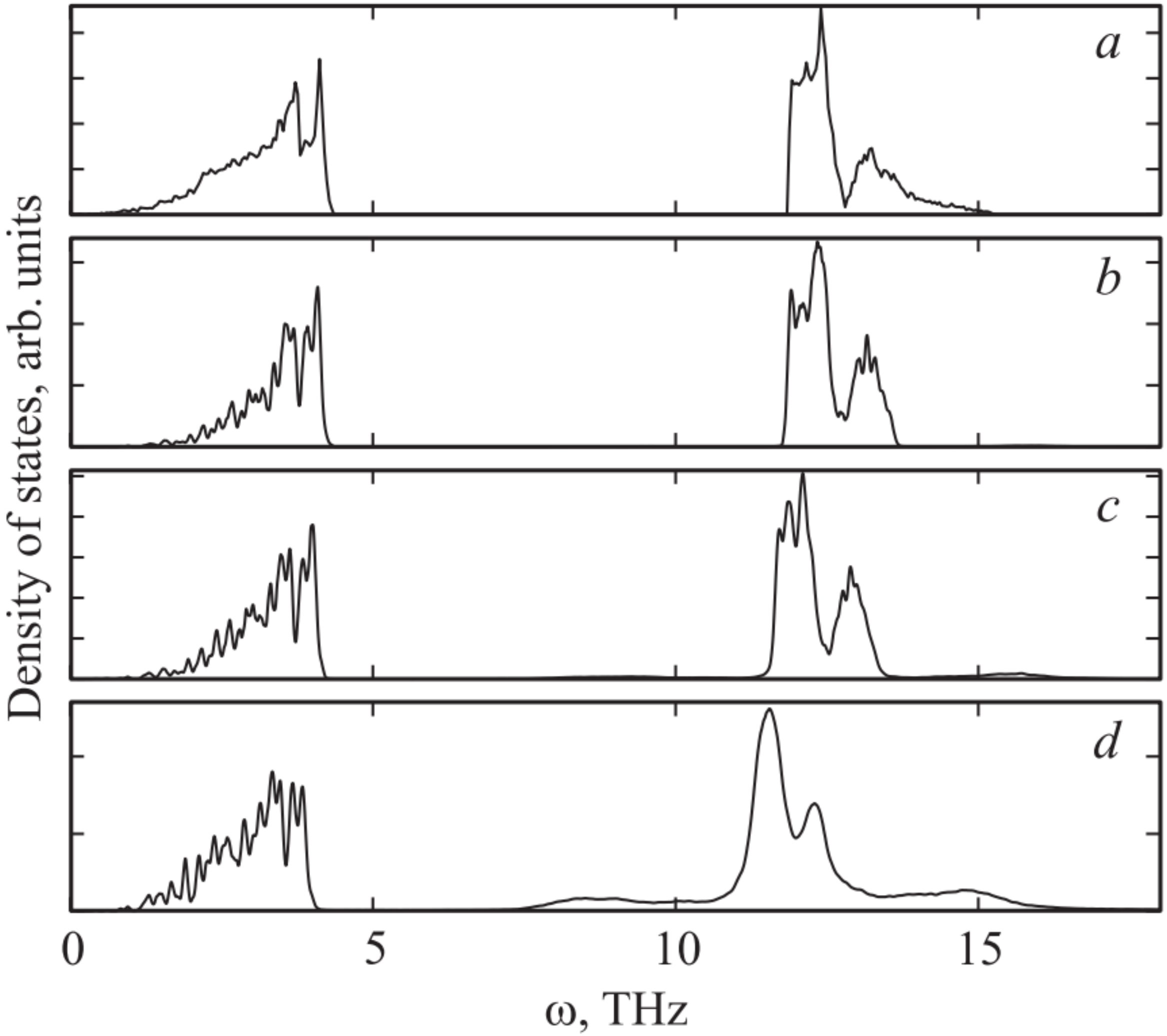


T = 0 K

T = 155 K

T = 310 K

T = 620 K

Morse pairwise potentials have been used for MD modeling

L. Khadeeva and S. Dmitriev, **Lifetime of gap discrete breathers in diatomic crystals at thermal equilibrium**, PHYS REV B **84**, (2011)

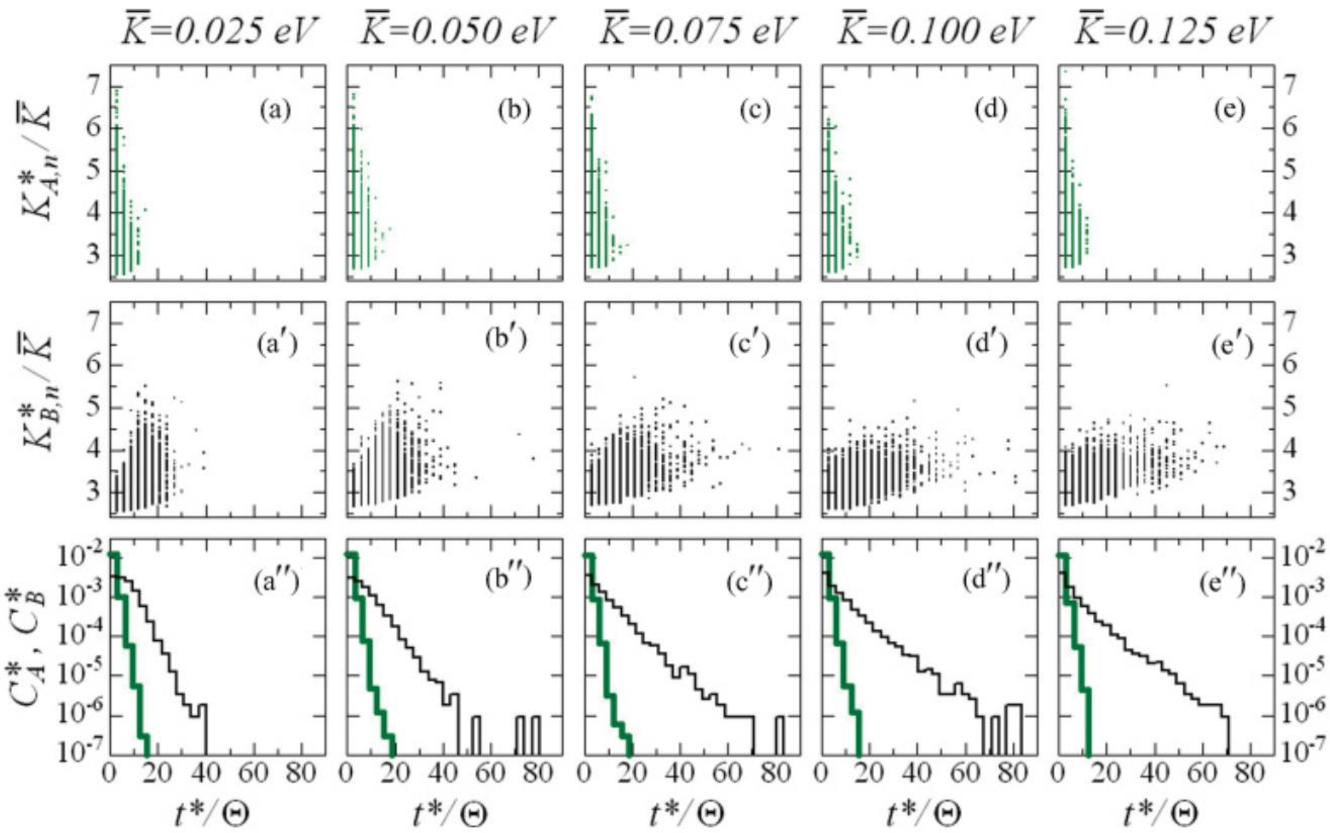


FIG. 5. (Color online) Characteristics of high-energy atoms in the crystal with atomic weight ratio $M_B/M_A = 0.10$. Rows correspond to five energies, $\overline{K} = \{0.025, 0.05, 0.075, 0.1, 0.125\}$ eV. (a)–(e) Relative energy of heavy atoms in high-energy state, $K^*_{A,n}/\overline{K}$, as a function of lifetime of this state, $t^*/\Theta$; (a′)–(e′) same as in (a)–(e), but for light atoms; (a″)–(e″) concentrations of high-energy heavy atoms, $C^*_A$ (thick line), and high-energy light atoms, $C^*_B$ (thin line), as functions of their lifetime, $t^*/\Theta$. The ordinate is given in logarithmic scale.

Morse pairwise potentials have been used for MD modeling

# NiH lattice (not deformed) at different T

As the temperature rises, low frequencies begin to predominate, which is apparently connected with the destruction of the hydride lattice and the increase in the mean free path of hydrogen atoms, which begin ‘free motion’ inside the lattice.

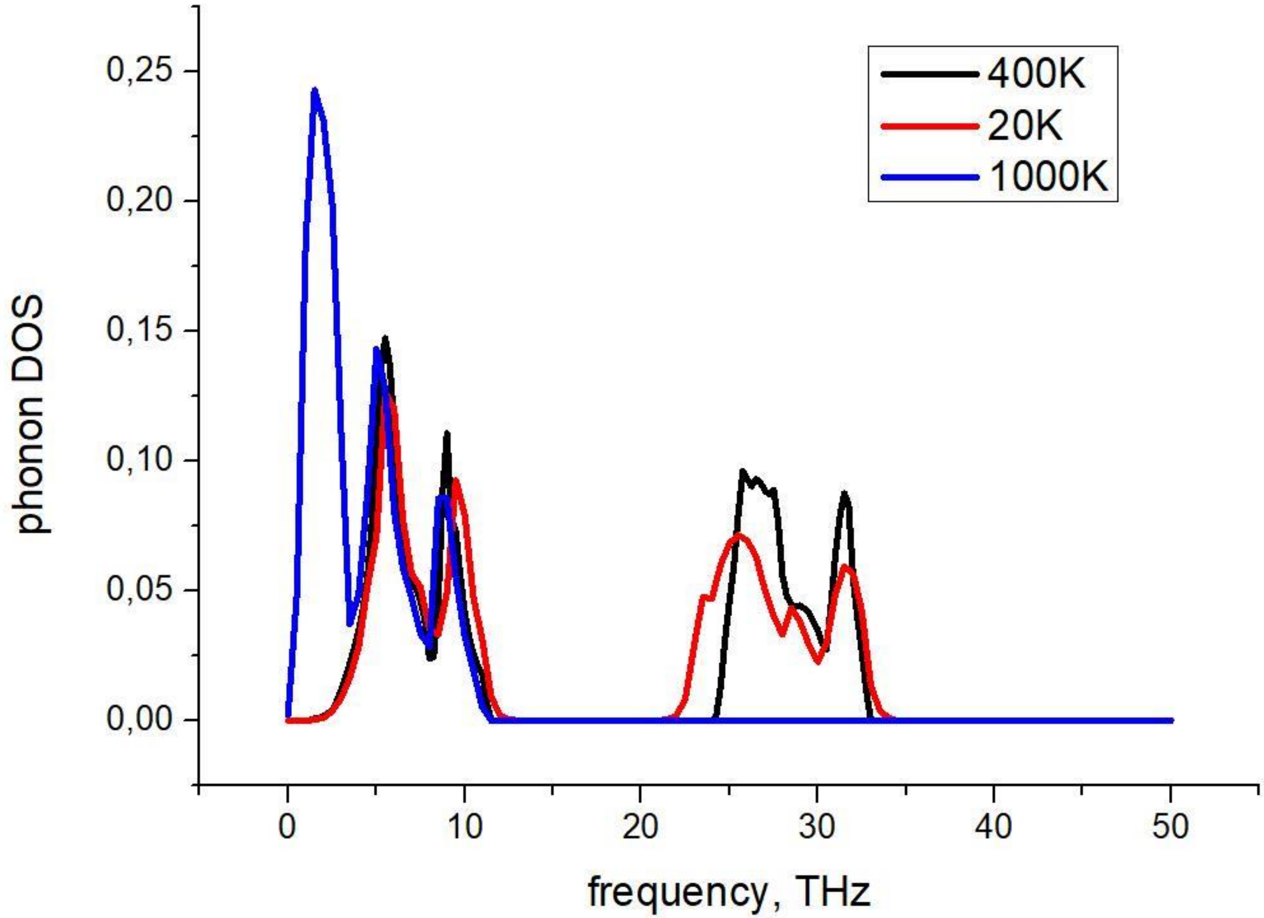

# Compressed (on 10%) PdH lattice at T=620K and T=1000K

With increasing T the phonon density shifts somewhat to the high-frequency region but no ‘shoulder’ appears in the gap.

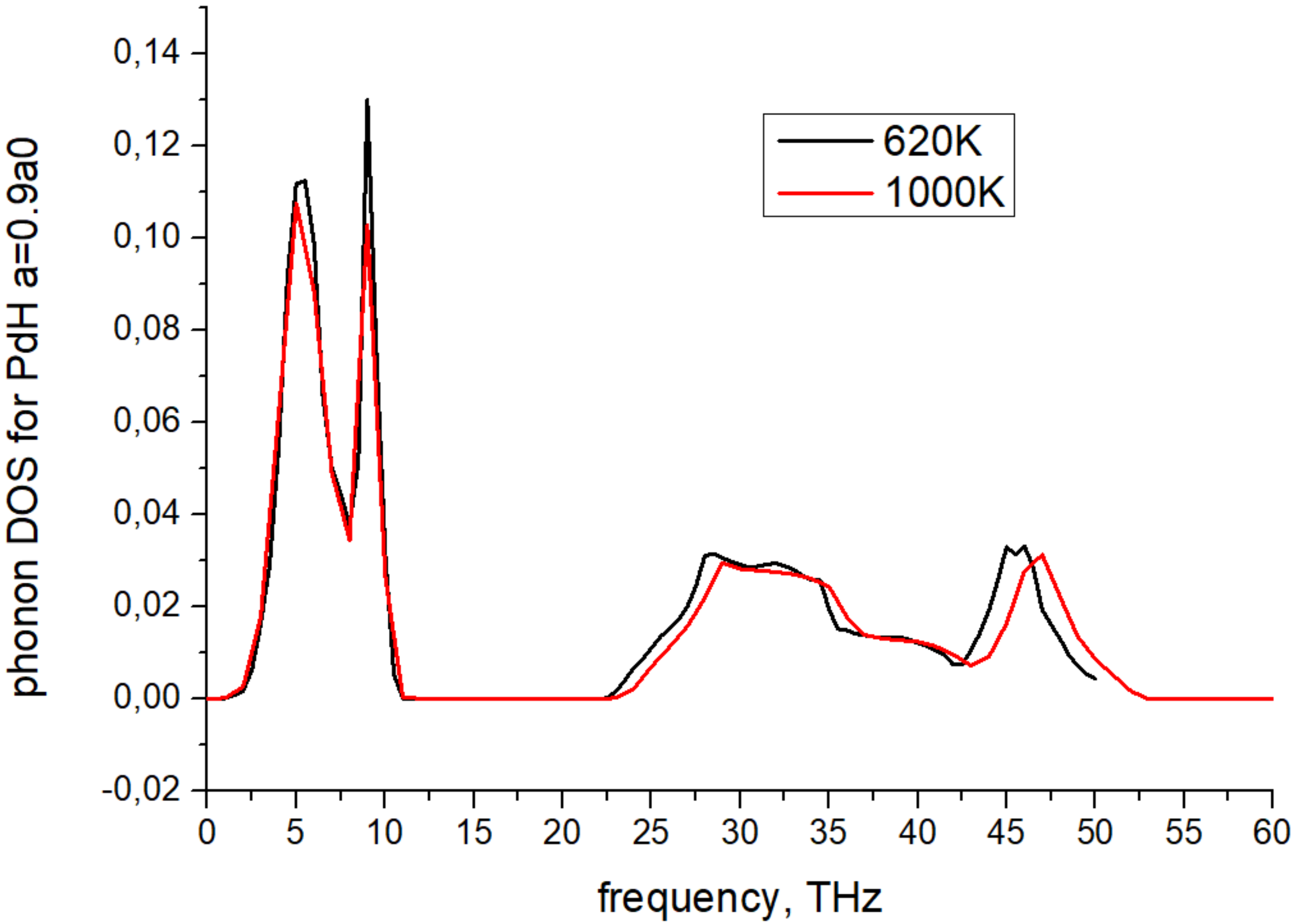

# Compressed (on 10%) NiH lattice at T=20K and T=1240K

As the temperature rises, low frequencies begin to predominate, which is apparently connected with the destruction of the hydride lattice and the increase in the mean free path of hydrogen atoms, which begin the ‘free motion’ inside the lattice.

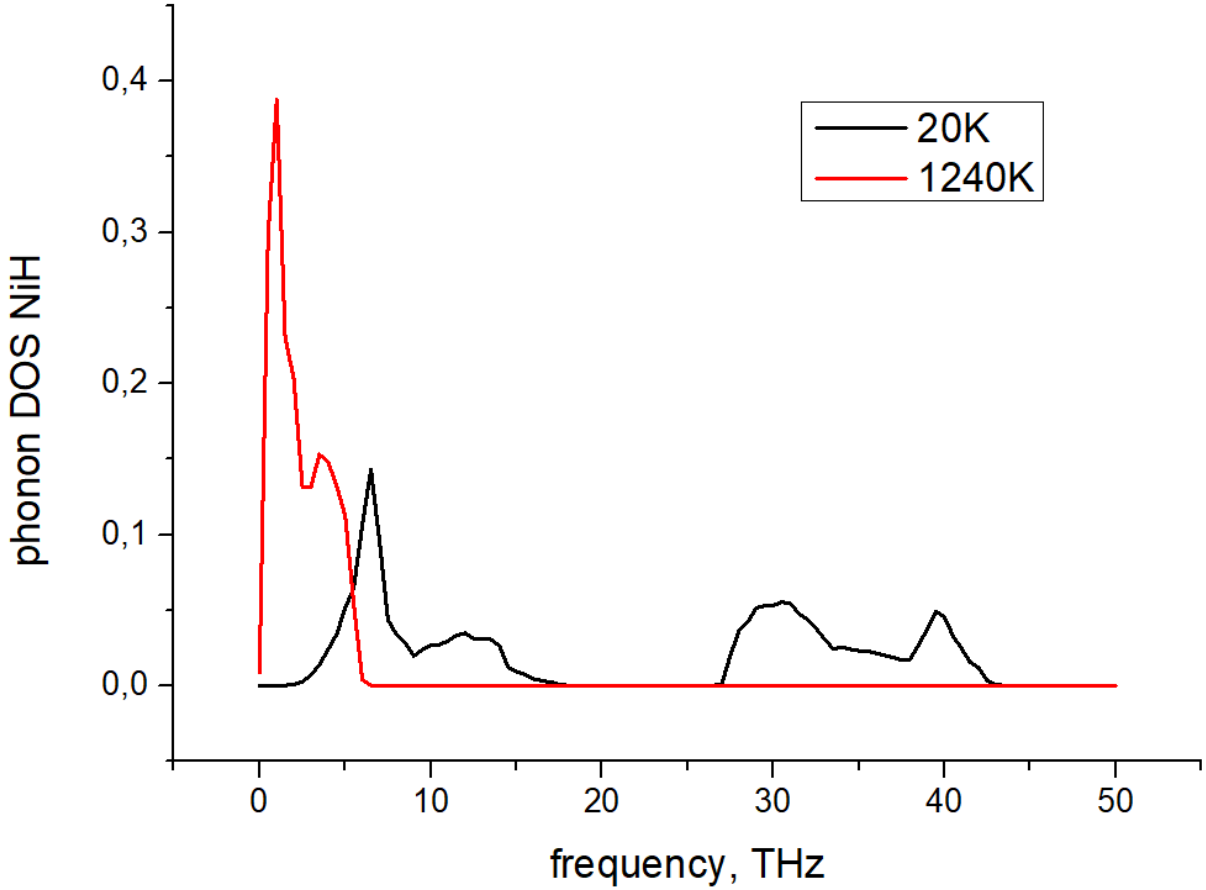

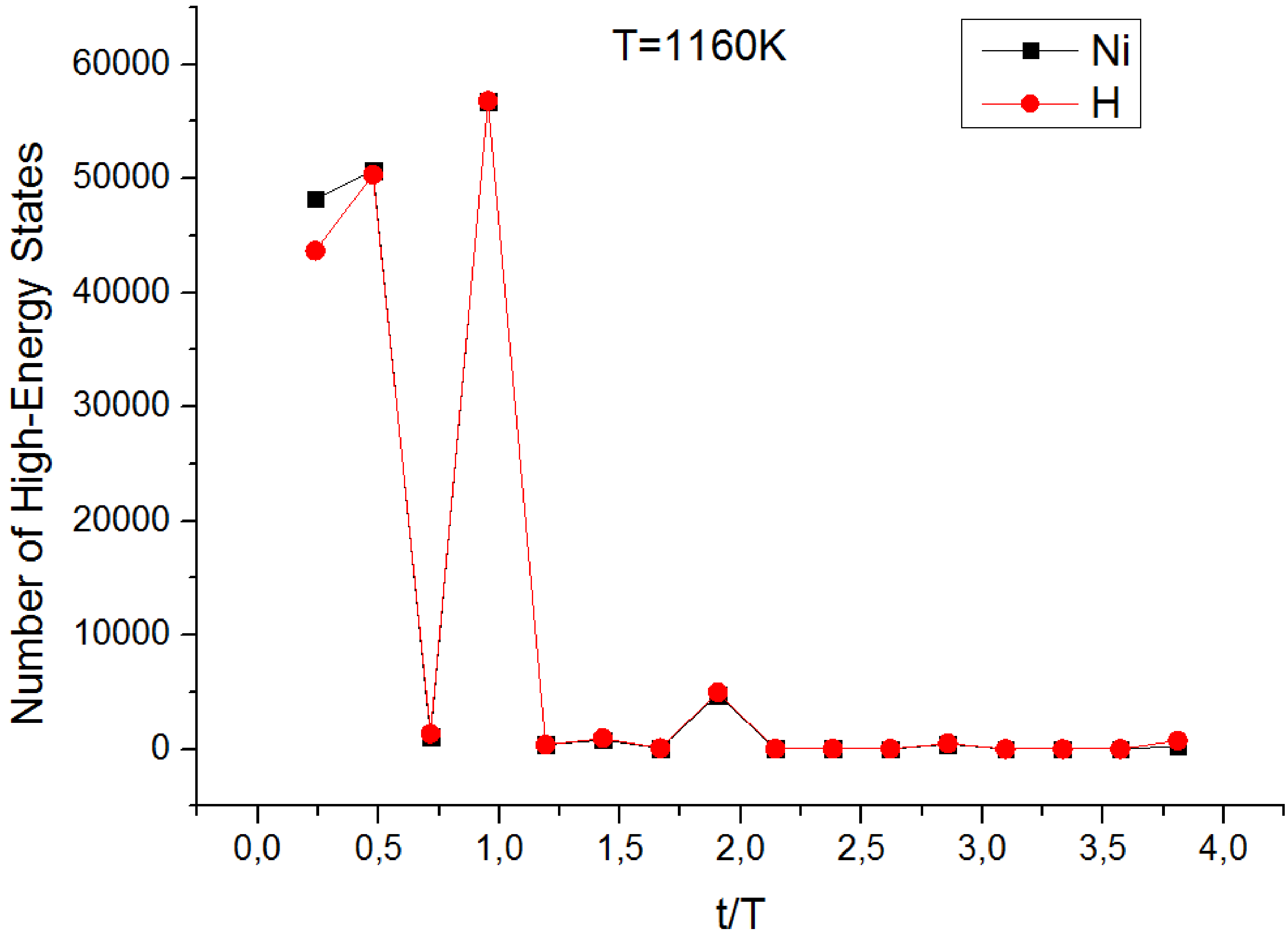


NiH MD modeling in LAMMPS package

## NiH lattice at T=1160K. High energy oscillations

Data for some arbitrary H atom in the Lattice

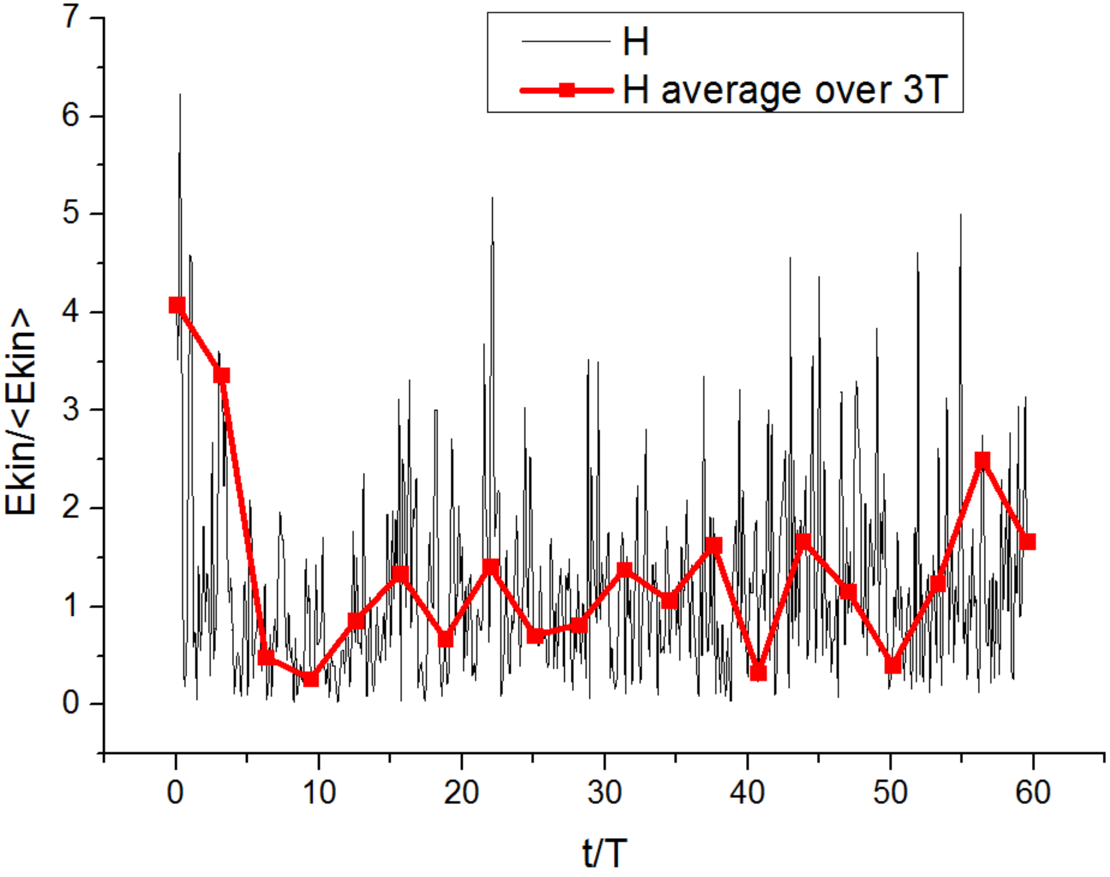


NiH MD modeling in **LAMMPS** package

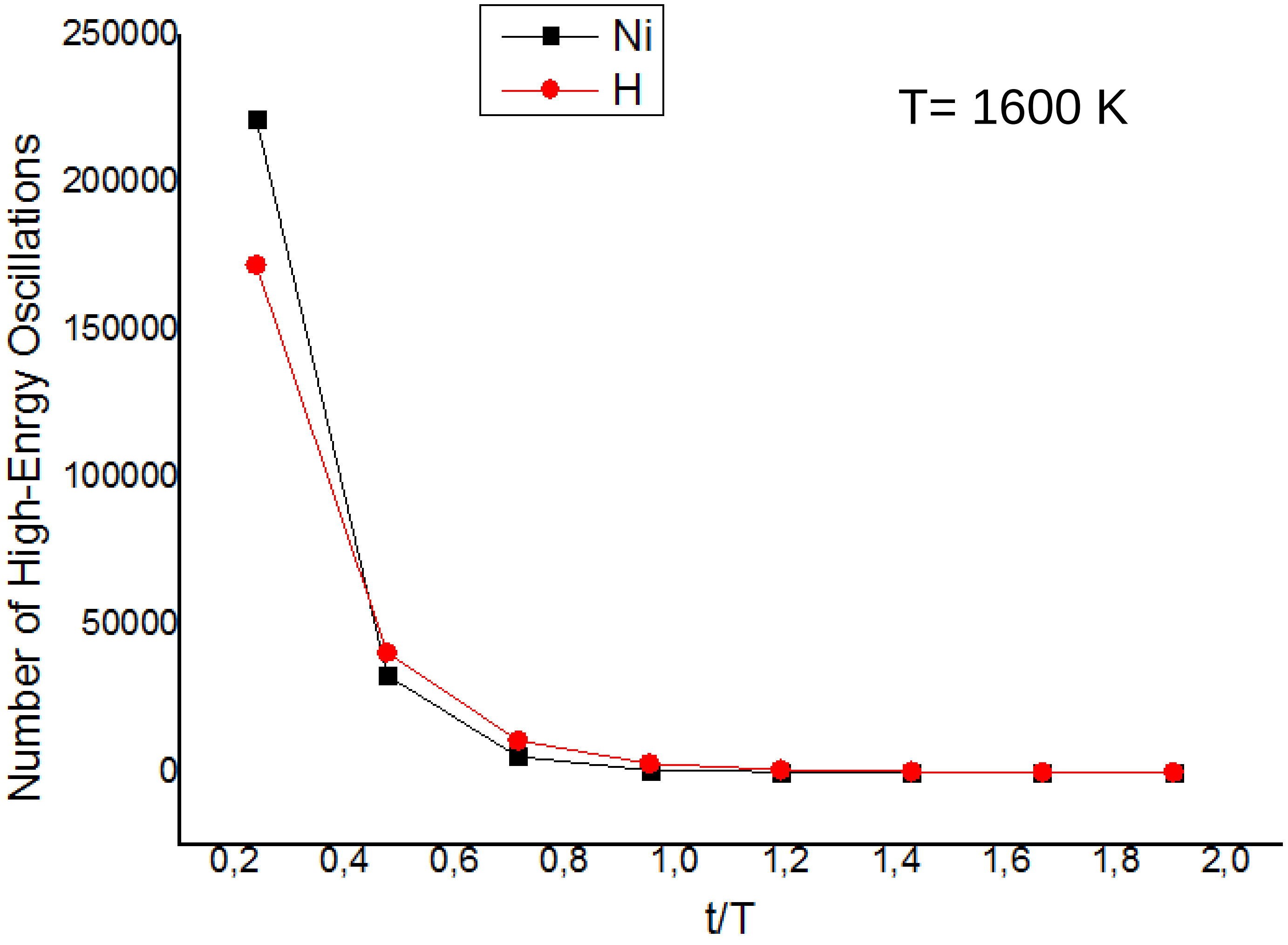


NiH MD modeling in **LAMMPS** package

# Magic Clusters

**magic clusters** (rus. кластеры, магические) — clusters of certain ("magic") sizes, which, due to their specific structure, have higher stability as compared to clusters of other sizes.

Number of atoms in the icosahedral cluster

$$n = (2N + 1) + 10\sum_{k=1}^{N} k^2$$

$$n = 13, 55, 147, 309, 561$$

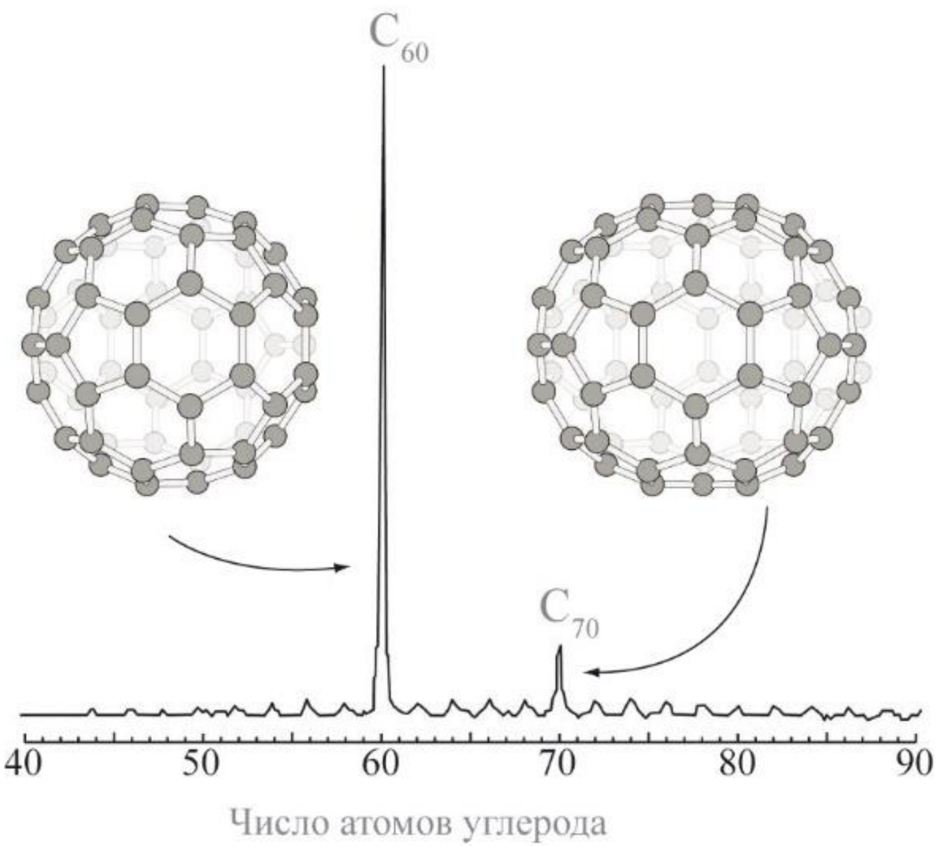


Mass spectrum of carbon clusters produced by laser evaporation of graphite. The highest peak corresponds to $C_{60}$ fullerene molecules, and the less intensive peak represents $C_{70}$ molecules

# Quasi-crystaline Pd cluster

E0=0.1eV

Cluster of 13 Pd atoms with quasi-crystalline $5^{th}$ order symmetry axis.

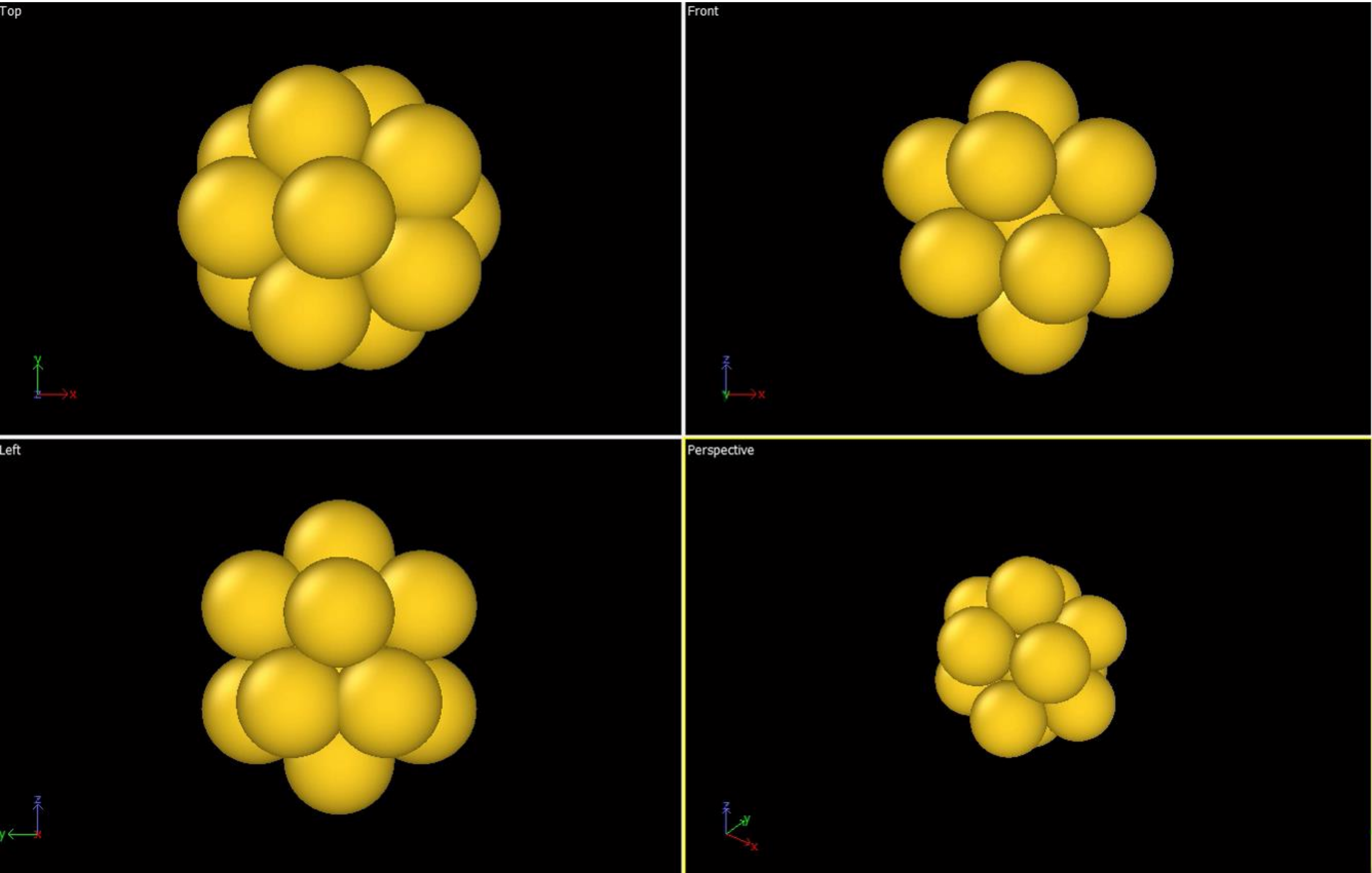

# 3d breather in a Magic cluster of 55 Pd atoms

with quasicrystalline $5^{th}$ order symmetry axis.

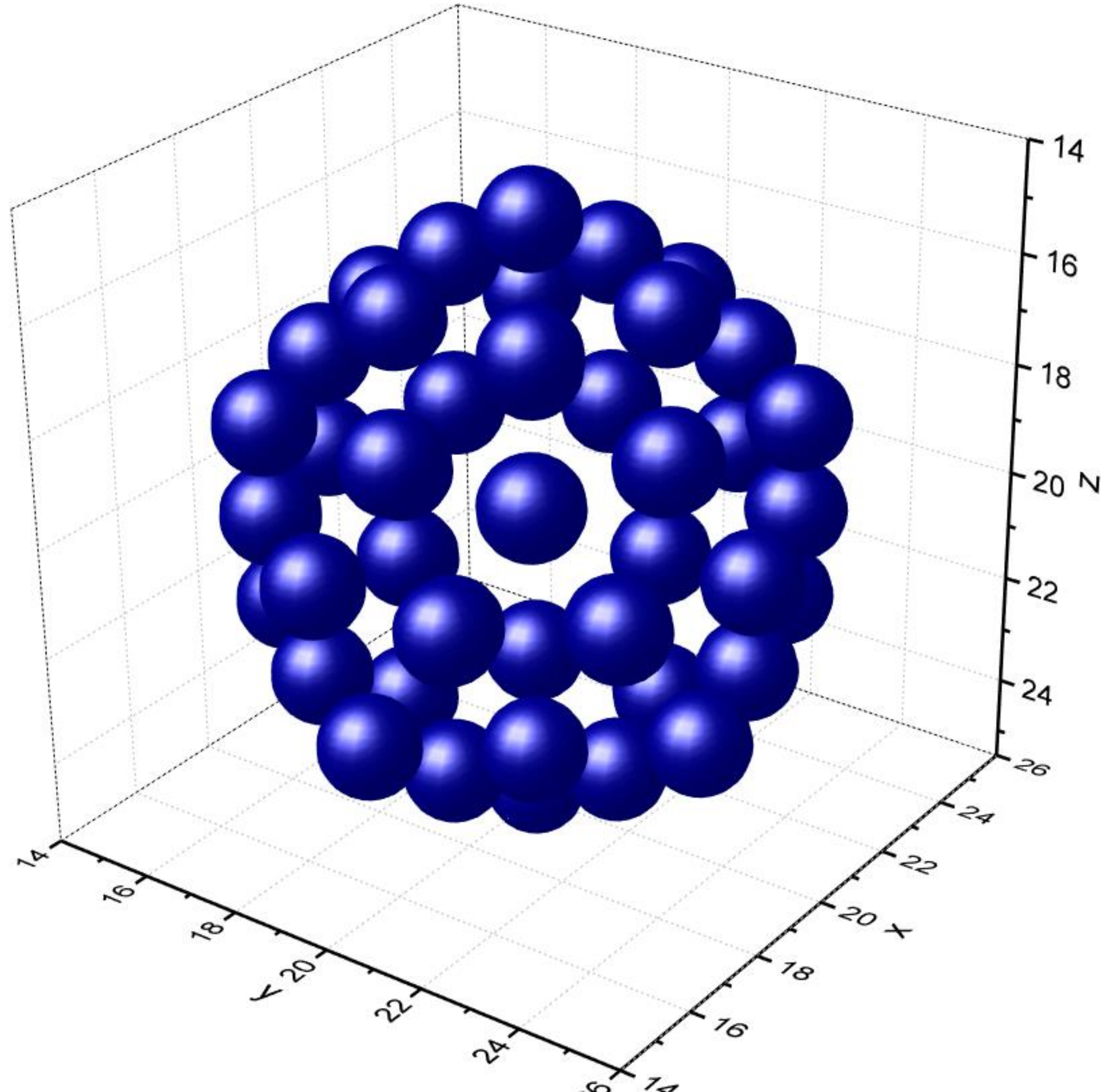

# Icosahedral cluster of 55 Pd atoms

**Initial conditions**: at the initial time moment all particles have zero displacements from equilibrium positions.

Atom #1 has initial kinetic energy **1.5**eV in [00-1] direction.

Atom #12 has initial kinetic energy **1.5**eV in [001] direction

**Boundary conditions**: free surfaces of cluster

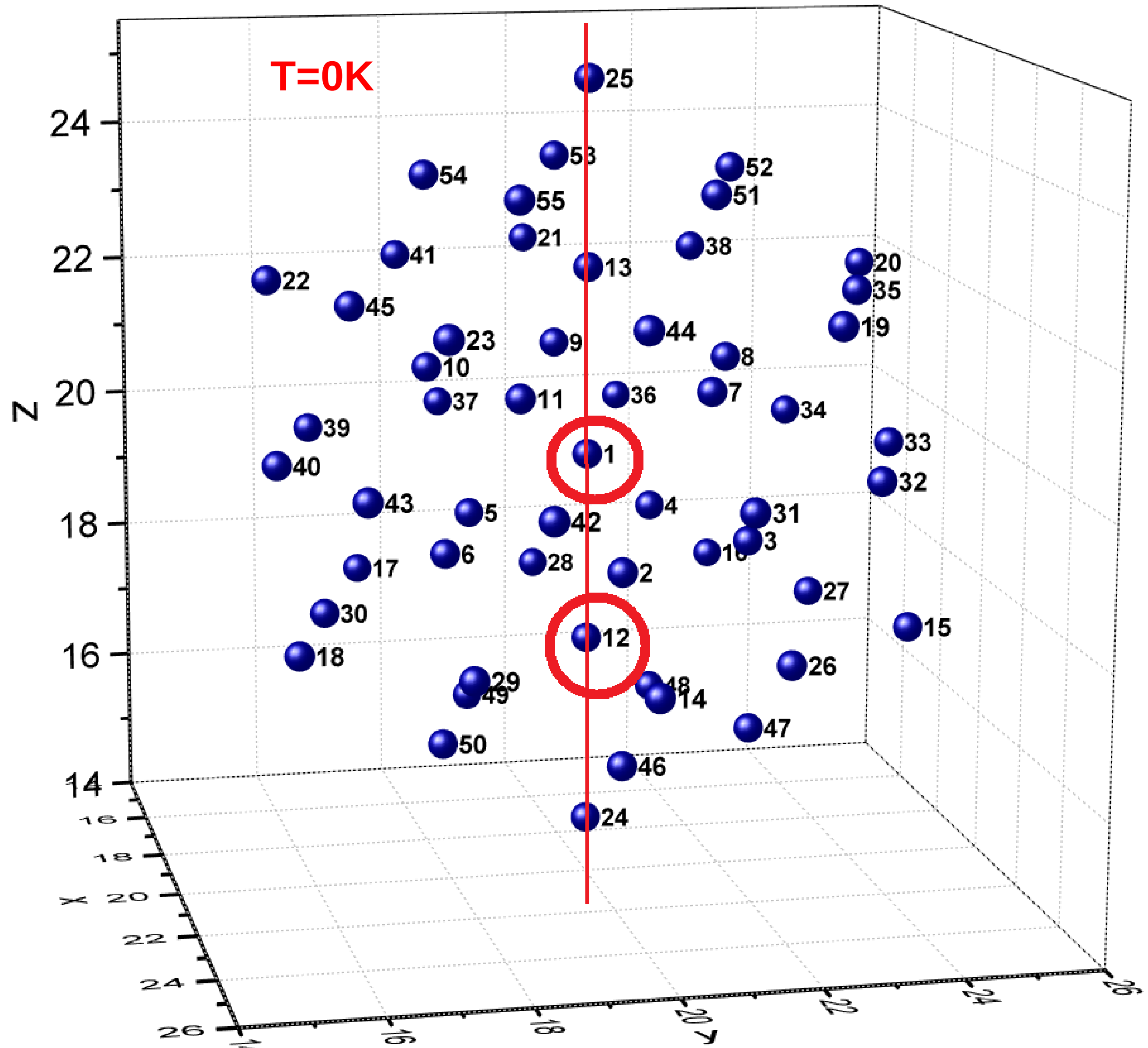

# Dynamics of the icosahedral cluster of 55 Pd atoms

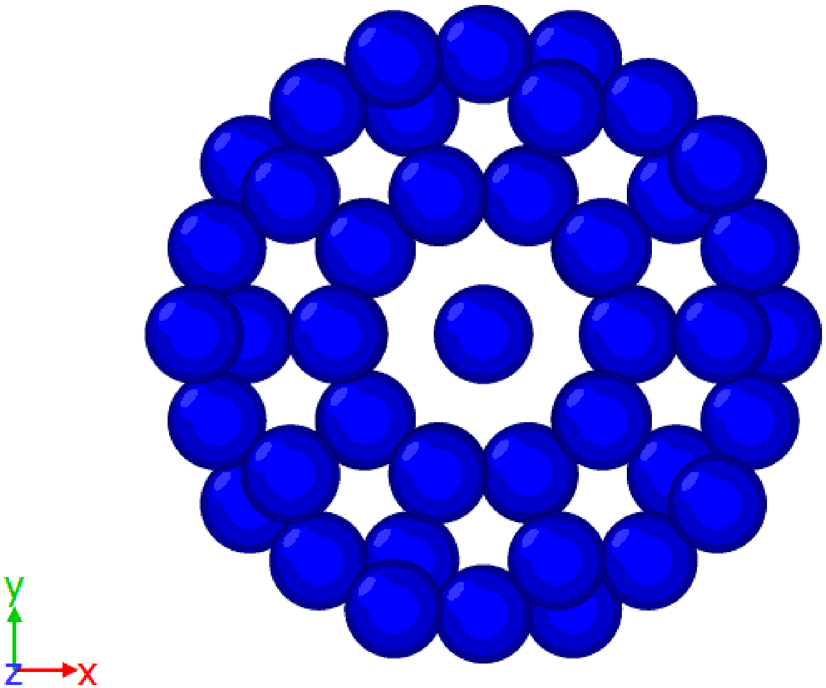


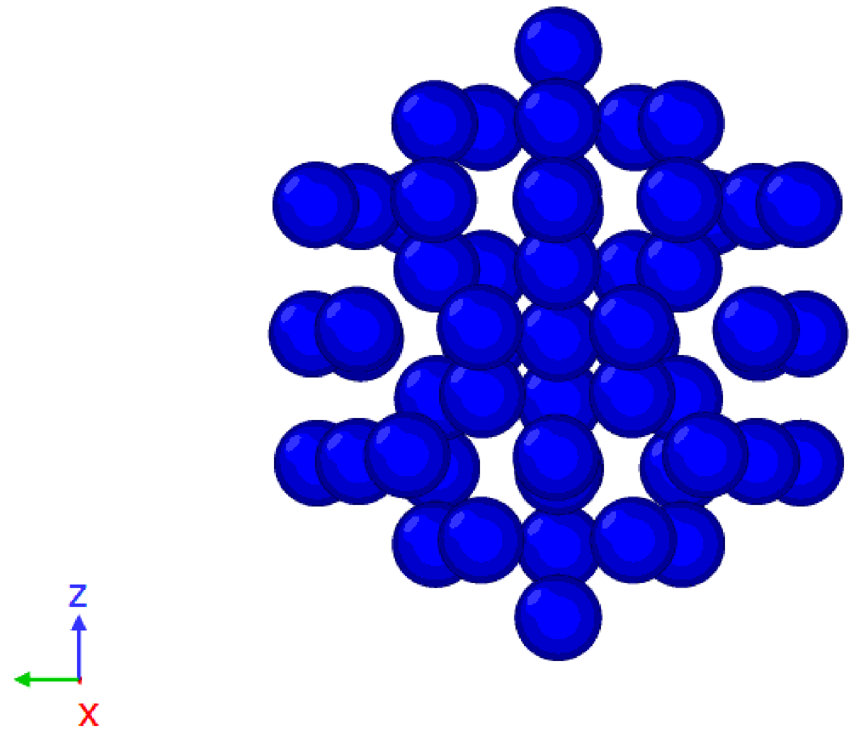


**It is seen from the visualization, that Localized Anharmonic Vibration is generated. The observed LAV in the atomic cluster represents the coherent collective oscillations of Pd atoms along quasi-crystalline symmetry directions.**

# Dynamics of the Pd atomic cluster

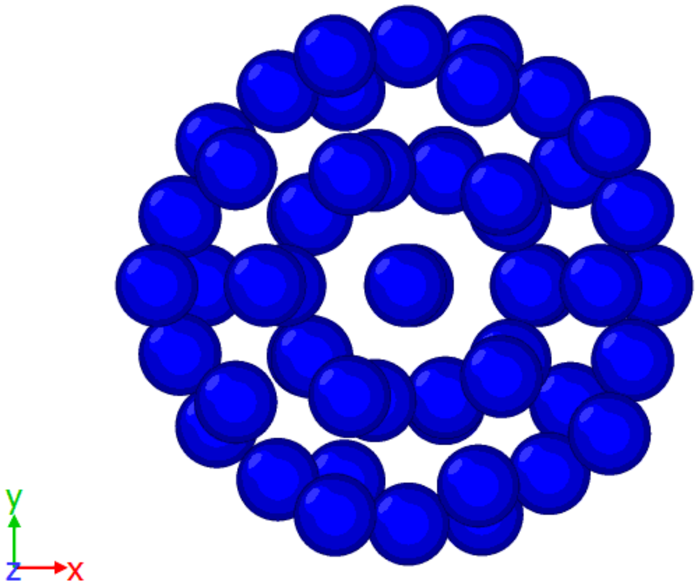


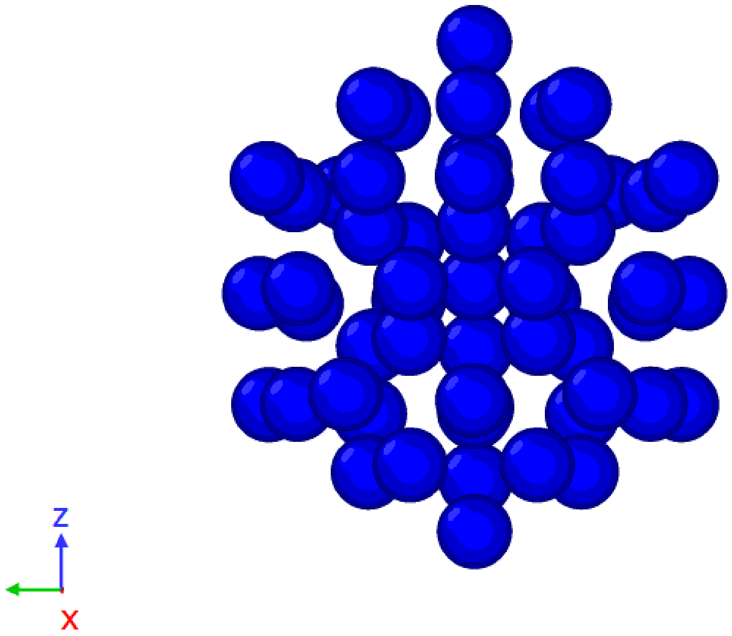


**If the initial energy, given to cluster is large enough (greater then the cohesive energy) then the cluster is destroyed after a certain period of time (~ ps) .**

# Conclusions and outlook

**New mechanism** of catalysis in solids is proposed, based on **time-periodic driving** of the potential landscape induced by *DB* s.

At high T, DBs may result in effective lowering of the reaction activation barrier.

At low T, DBs may result in increasing energy of Zero Point Vibrations enhancing the tunneling through the potential barrier

**Outstanding problems**:

Existence and properties of LAV at elevated temperatures

Account of quantum effects in MD/DFT at low temperatures

Experimental verification of the proposed concept

# Publications


1. V.I. Dubinko, P.A. Selyshchev and F.R. Archilla, *Reaction-rate theory with account of the crystal anharmonicity*, **Phys. Rev. E** 83 (2011**),**041124-1-13
2. V.I. Dubinko, F. Piazza, *On the role of disorder in catalysis driven by discrete breathers*, **Letters on Materials** 4 (2014) 273-278.
3. V.I. Dubinko, *Low-energy Nuclear Reactions Driven by Discrete Breathers*, **J. Condensed Matter Nucl. Sci**., 14, (2014) 87-107.
4. V.I. Dubinko, *Quantum tunneling in gap discrete breathers*, **Letters on Materials**, 5 (2015) 97-104.
5. V.I. Dubinko, *Quantum Tunneling in Breather 'Nano-colliders'*, **J. Condensed Matter Nucl. Sci.**, 19, (2016) 1-12.
6. V. I. Dubinko, D. V. Laptev, *Chemical and nuclear catalysis driven by localized anharmonic vibrations*, **Letters on Materials** 6 (2016) 16–21.
7. V. I. Dubinko, *Radiation-induced catalysis of low energy nuclear reactions in solids***, J. Micromechanics and Molecular Physics**, 1 (2016) 165006 -1-12.
8. V. I. Dubinko, D. V. Laptev, A. S. Mazmanishvili, J. F. R. Archilla*, "Quantum dynamics of wave packets in a nonstationary parabolic potential and the Kramers escape rate theory", J. Micromechanics and Molecular Physics*, **1**, 650010 -1-12 (2016)
9. Dubinko V., Laptev D., Irwin K., Catalytic mechanism of LENR in quasicrystals based on localized anharmonic vibrations and phasons, **J. Condensed Matter Nucl. Sci.** -2017.-V. 24.- P. 1-12

THANK YOU
FOR YOUR ATTENTION!

$$\langle E \rangle_{theor}(t) \approx \text{h}\omega_0 \left( n + \frac{1}{2} \right) \cosh \frac{g\omega_0 t}{2}$$

$g << 1$

**General case: n = 0,1,2, …**

$$\langle E \rangle_{num}(t) = \frac{\hbar\omega_0}{2} \left( n + \frac{1}{2} \right) \left[ \frac{\dot{Y}^2 + \omega_0^2 \dot{Z}^2}{\omega_0^2} + \frac{\omega^2(t)}{\omega_0^2} \left( Y^2 + \omega_0^2 Z^2 \right) \right]$$

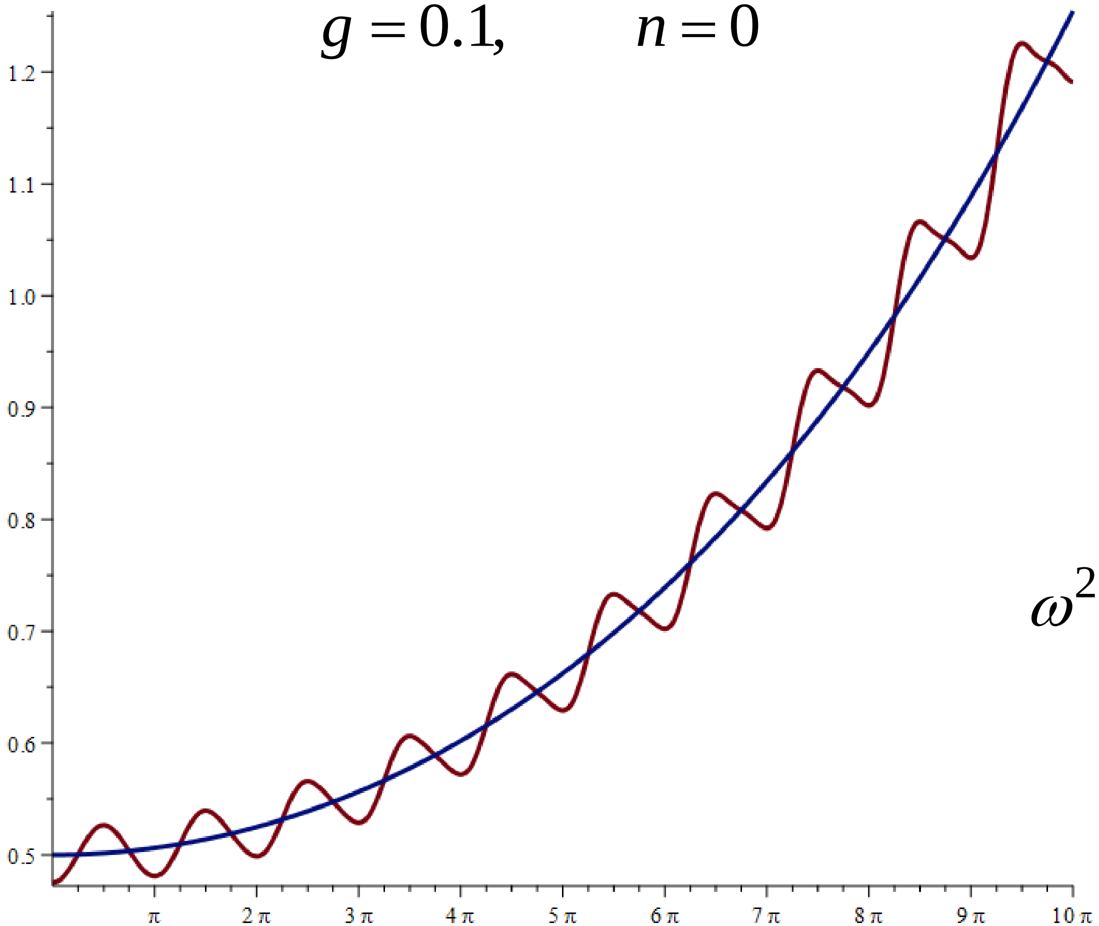


$$\begin{cases} \ddot{Y}(t) + \omega^2(t) Y(t) = 0 \\ \dot{Y}(0) = 0, \qquad Y(0) = 1 \end{cases}$$

$$\begin{cases} \ddot{Z}(t) + \omega^2(t) Z(t) = 0 \\ \dot{Z}(0) = 1, \qquad Z(0) = 0 \end{cases}$$

$$\omega^2(t) = \omega_0^2 \left[ 1 - g \cos(2\omega_0 t) \right]$$

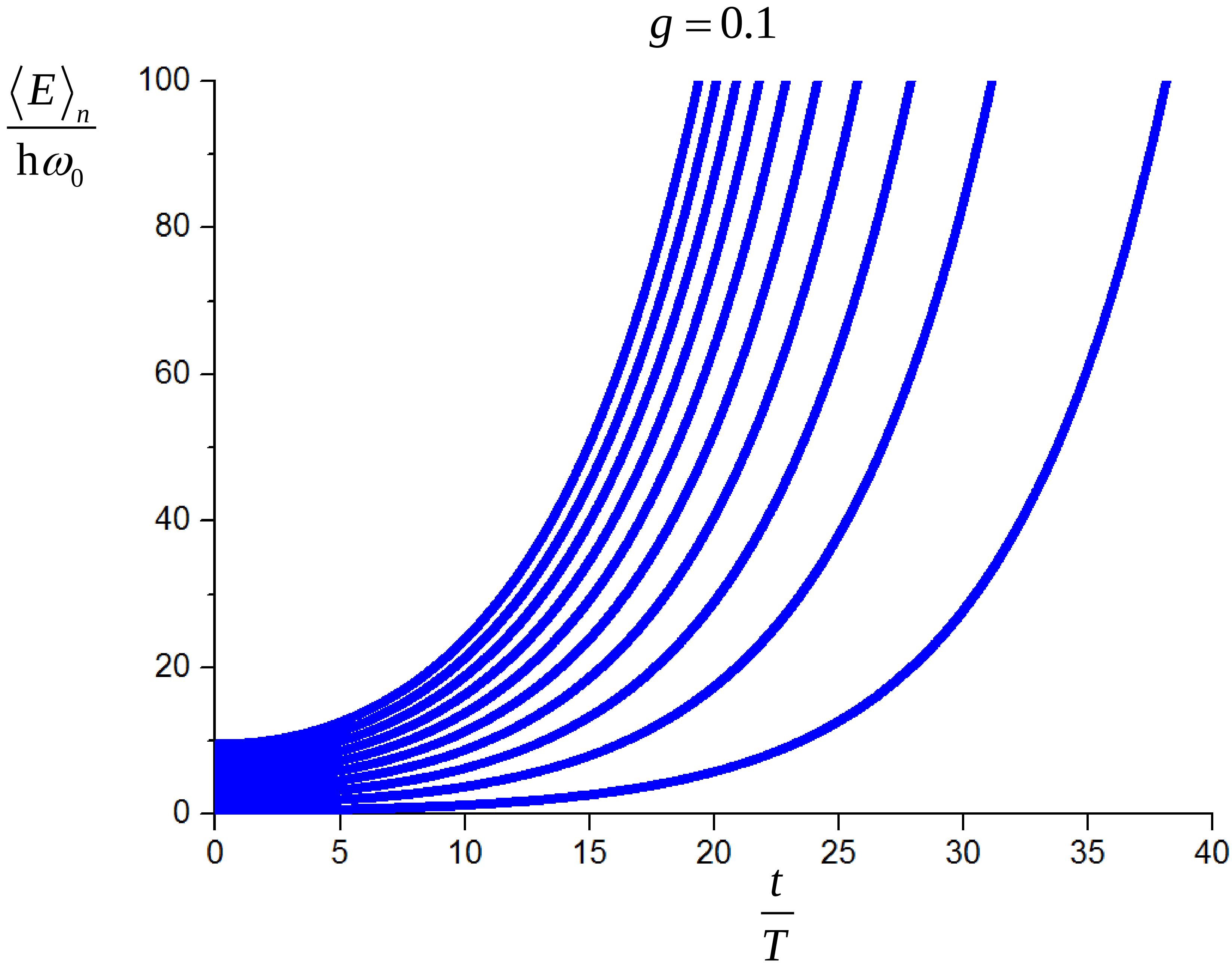

$g = 0.1$
$\frac{\langle E \rangle_n}{\hbar\omega_0}$
100
80
60
40
20
0
0
5
10
15
20
25
30
35
40
$\frac{t}{T}$